SYNTACTIC FOAM DEVELOPMENT FOR USE IN THIRD-GENERATION LINER-STYLE HYDRAULIC SUPPRESSORS

A Thesis
Presented to
The Academic Faculty

by

Nathaniel Robert Pedigo

In Partial Fulfillment
of the Requirements for the Degree
Masters of Science in Mechanical Engineering in the
George W. Woodruff School of Mechanical Engineering

Georgia Institute of Technology
December 2017

SYNTACTIC FOAM DEVELOPMENTS FOR USE IN THIRD-GENERATION LINER-STYLE HYDRAULIC SUPPRESSOR

Approved by:

Dr. Kenneth A. Cunefare, Advisor
Woodruff School of Mechanical Engineering
Georgia Institute of Technology

Dr. Laurence Jacobs
College of Engineering
Georgia Institute of Technology

Dr. Wayne Book
Woodruff School of Mechanical Engineering
Georgia Institute of Technology

Date Approved: December 06, 2017

ACKNOWLEDGEMENTS

I would like to acknowledge the many people who helped me to complete this work. First, I would like to thank my parents, Ryan and Leslie Pedigo, and my sister, Christen Pedigo, for their ceaseless support. I would also like to express my gratitude to my lab mates Elliott Gruber, Fahad Vora, Kamil Kocak, Gregor Wettermann, and others who have provided both technical support and friendship. Thanks must be given to the sponsors of my research, Wilkes & Mclean Ltd. and Danfoss, without whose support I would not have been able to undertake this research. I would also like to thank the members of my reading committee, Dr. Laurence Jacobs and Dr. Wayne Book. Finally, thanks must be given to my advisor, Dr. Kenneth Cunefare, who has offered significant academic guidance, vital support for this research, and encouraged my growth as an engineer.

TABLE OF CONTENTS

LIST OF TABLES

LIST OF FIGURES

LIST OF SYMBOLS AND ABBREVIATIONS

A	Complex wave amplitude of positive directed travelling plane wave in the upstream section of pipe or cross-sectional area of a pipe; as a subscript, denotes Side A of polyurethane
a	Inner radius of the pipe in the test section
Adj	Mass adjustment
B	Complex wave amplitude of negative directed travelling plane wave in the upstream section of pipe; as a subscript, denotes Side B of polyurethane
$burst$	Subscript used to denote a bursting condition
$collapse$	Subscript used to denote a collapsing condition
c	Speed of sound
c_{phase}	Phase speed of sound
cr	Subscript used to denote critical
C_{xy}	Coherence between sensors x and y
$downstream$	Subscript used to denote downstream condition
Δ	Change
E	Young's modulus, or complex wave amplitude of forward directed travelling plane wave in the downstream section of pipe
EW	Effective weight
ext	Subscript used to denote external condition
f	frequency
F	Complex wave amplitude of negative directed travelling plane wave in the downstream section of pipe
$foam$	Subscript used to denote foam property
F_v	Volume fraction of voids at a given pressure
G	Shear modulus

G_{xy}	Spectral density between signals at sensors x and y
γ	Complex wave number
H_{hi}	Transfer function between signals at sensors h and i
Hz	Hetz [cycles/s]
i	Subscript used to denote inner
IMP	Initial Microsphere Pressurization, this is a gage pressure
int	Subscript used to denote internal condition
j	The imaginary number, $\sqrt{-1}$
j'	Extrema of a Bessel function
J	Bessel function
K	Bulk modulus
k_{lm}	Wavenumber corresponding to mode lm
L	Length of the liner
λ	Wavelength
MDI	Methylene diphenyl diisocyanate
MPa	Megapascals
m	Mass
μ	Fluid viscosity
μS	Subscript used to denote microsphere(s)
%NCO	Measure of the content of isocyanate
v	Poisson's ratio
o	Subscript used to denote outer
oil	Subscript used to denote oil property
OH#	Measure of the hydroxyl group content of a polyol
ω	Angular frequency

ω_{lm}	Cutoff frequency for waves of mode lm
P	Static or differential pressure
p	Dynamic (acoustic) pressure
psig	Pounds per square inch, gage
PTMEG	Polytetramethylene ether glycol
Q	Volume flow rate
r	Radius
rpm	Revolutions per minute
r_w	Average microsphere wall radius
ρ	Density
sys	Subscript used to denote system
σ_{yield}	Yield stress of the microsphere
t	Time; as a subscript, denotes transmitted
t_w	Wall thickness of the microsphere
t_{xy}	Transfer matrix element located at row x, column y
t_v	Viscous boundary layer thickness
T_g	Glass transition temperature
TL	Transmission loss
torr	Unit of vacuum measurement, 1 torr = 1/760 atm
u	Acoustic particle velocity or a subscript used to denote urethane property
upstream	Subscript used to denote upstream condition
V	Volume
v	Subscript used to denote void
VF	Initial volume fraction of microspheres in syntactic foam
w	Subscript used to denote a dimension of the microsphere wall

W	Acoustic energy
$WT\%$	Weight percent
x	Position in test section
Z_0	Specific acoustic impedance
1	Subscript used to denote initial state
*	Superscript used to denote effective material property

SUMMARY

A third-generation of in-line, liner-style hydraulic suppressors was developed that takes advantage of advancements of syntactic foam technology. The chemistry of the developed liner was varied so that the acoustic properties of the foam could be retained when repetitively exposed to the extremes of the hydraulic environment. The developed liner uses microspheres that can be charged to an elevated initial microsphere pressurization which results in an increased acoustic performance at elevated system pressures. The developed liner also addresses the limitations of the first and second-generation liner-style suppressors in terms of initial volume fraction of microspheres, allowing for enhanced acoustic performance over broad pressure ranges.

Acoustic diffusers, necessary for bladder-style in-line hydraulic suppressors, were considered for use with liner-style hydraulic suppressors. It was found that acoustic suppressors are not appropriate for use in liner-style suppressors due to the possible dimensional changes of the liner under hydrostatic loading.

Testing indicates that increasing the initial microsphere pressurization and the initial volume fraction of microspheres significantly increases the acoustic performance of the suppressors. Additional testing indicates that the host matrix composition can be refined so that the acoustic performance is stable over multiple exposures to elevated temperature and pressure. Using the results of the testing, a suggestion for an improved formulation of syntactic foam is made.

CHAPTER 1. INTRODUCTION

Fluid-borne noise, often referred to as pressure ripple in the hydraulics industry, is a ubiquitous problem in the hydraulics industry, decreasing equipment life and increasing the ambient noise level. Fluid-borne noise will couple with the structural components of a hydraulic system, which can introduce significant fatigue cycles to the system components about the static stress induced by the system pressure. These fatigue cycles are particularly critical at the least durable components in the system such as seals and valves, where O-ring wear can lead to leaks.

Fluid-borne noise in hydraulic systems is generated by system components such as pumps and valves. Most hydraulic pumps produce intense tonal noise at the fundamental frequency of the pump and its harmonics. Valves in hydraulic systems tend to introduce broadband noise by restricting and directing the flow of oil, inducing turbulence. The spectral content of the fluid-borne noise in a representative hydraulic system at 10.3 MPa is shown in Figure 1. The strong tonal components of the noise were generated at the pump's passing frequency and its harmonics while the broadband noise was generated by turbulence induced in valves. It can be seen from Figure 1 that the amplitude of the fluid-borne noise can be on the order of 10% of the system pressure. This indicates that hydraulic systems may cause significant fatigue cycles in the system components. The performance requirements of these components generally prevent any redesigns that could mitigate noise production.

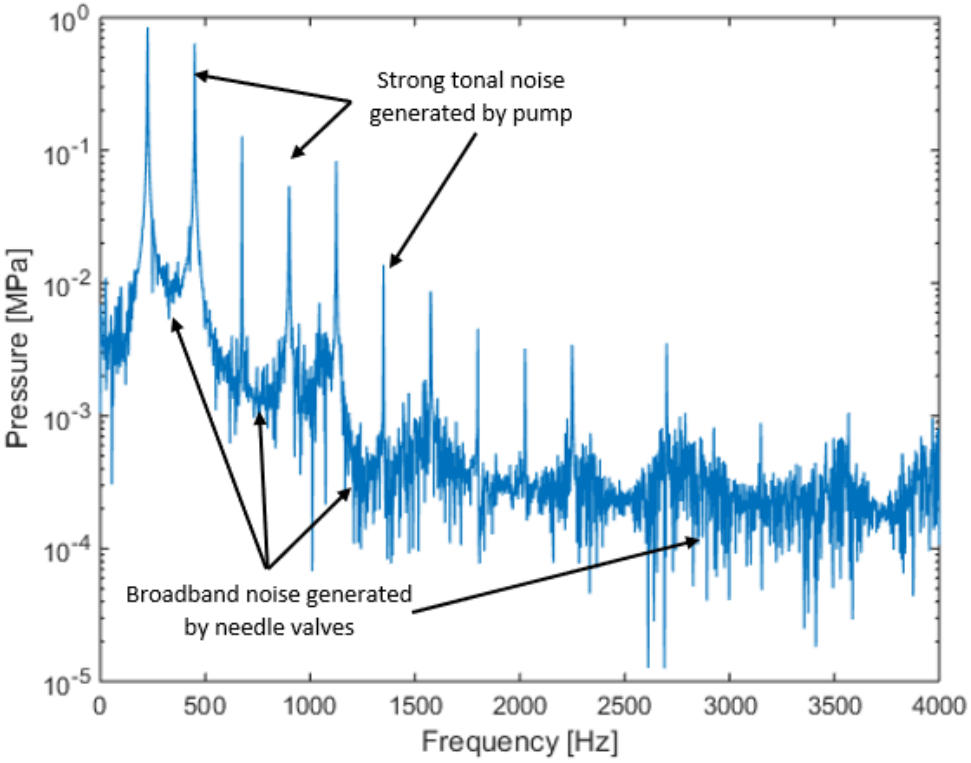

Figure 1 – Spectral content of the fluid-borne noise in a representative system with 10.3 MPa static pressure, exhibiting strong tonal characteristics corresponding to the harmonics of a 9-piston pump operating at 1500 rpm and with high levels of broadband noise induced by turbulence at a needle valve [1].

The structural-borne noise will couple with the surrounding air, increasing the ambient noise, potentially interfering with work site communications and/or leading to hearing loss. This breakout noise has been shown to be a significant factor when considering the purchase of new mobile equipment, following only adequate power and good fuel economy [2].

Many hydraulic systems are used in size limited applications, such as mobile, off-road equipment, an example of which can be seen in Figure 2. Because of the many size limited applications of hydraulics, a robust yet small device is needed to treat the fluid-borne noise. Conventional noise treatment solutions such as Helmholtz resonators and

expansion chambers require prohibitively large form factors in hydraulic applications due to the high speed of sound [1].

Figure 2 – Construction equipment is a typical mobile hydraulics application with size and weight restrictions.

1.1 Current State of the Art

Inline suppressors were developed to address the fluid-borne noise in hydraulic systems without significantly increasing the form factor of the system. Both bladder-style and liner-style suppressors treat noise by creating a mismatch in the specific acoustic impedance between the suppressor and the hydraulic system.

1.1.1 Bladder-Style Suppressor

Bladder-style suppressors contain a rubber bladder backed by pressurized gas, usually nitrogen, and restrained by a diffuser, as shown in Figure 3. The charge of the suppressor is determined by the system pressure for which the suppressor is being used.

Despite the high transmission losses (TL) achievable with this style of suppressor, the utility of bladder-style suppressors is limited by the required maintenance and potential for catastrophic failure. The diffuser serves a dual purpose in bladder style suppressors, both supporting the bladder and introducing acoustic damping to the suppressor.

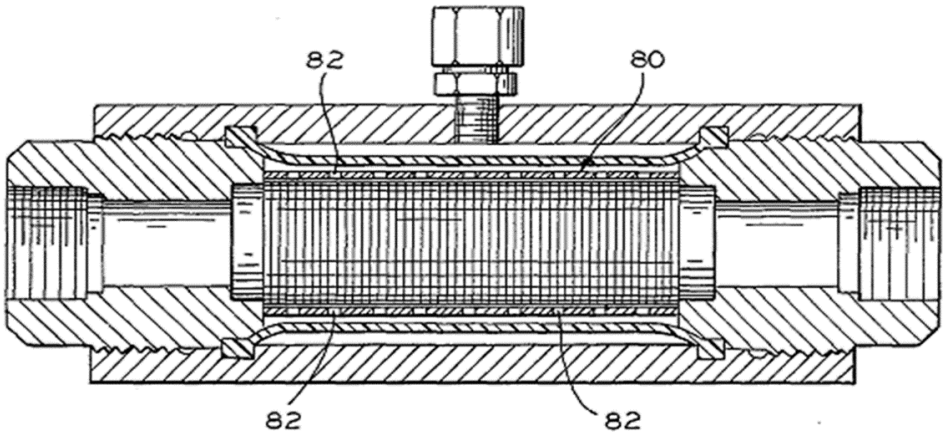

Figure 3 – Typical design of a bladder-style suppressor. The item marked as 80 is the rubber bladder; the item marked as 82 is the diffuser [3].

1.1.2 Liner-Style Suppressors

Liner-style suppressors use a syntactic foam composed of microspheres contained by a polymer bound within a host polymer. The liner-style suppressor is intended to be a maintenance free design; no charging is necessary, and the form of catastrophic failure experienced in the bladder-style suppressor is impossible. Table 1 describes the three generations of liner-style suppressors and the various defining characteristics of those generations. Figure 4 shows an example of a first-generation liner-style suppressor; the liner is an annular cylinder which allows the oil to flow unimpeded through the suppressor. Figure 5 shows an example of a second-generation liner-style suppressor; the shell of the suppressor and the use of a diffuser differs from that of the first-generation

suppressor. The third-generation of liner-style suppressors uses the same original equipment manufacturing (OEM) shell and lacks a diffuser.

Table 1 – Syntactic foam, liner-style hydraulic suppressor generations.

Generation	Material	Internal Components	Volume Fraction	Initial Microsphere Pressurization	Shell Form Factor
1	GR9-625	None	Fixed	Not Possible	OEM
2	GR9-625	Diffuser	Fixed	Not Possible	OEM
3	Various	None	Variable	Possible	OEM

Figure 4 – First generation of liner-style suppressor [4].

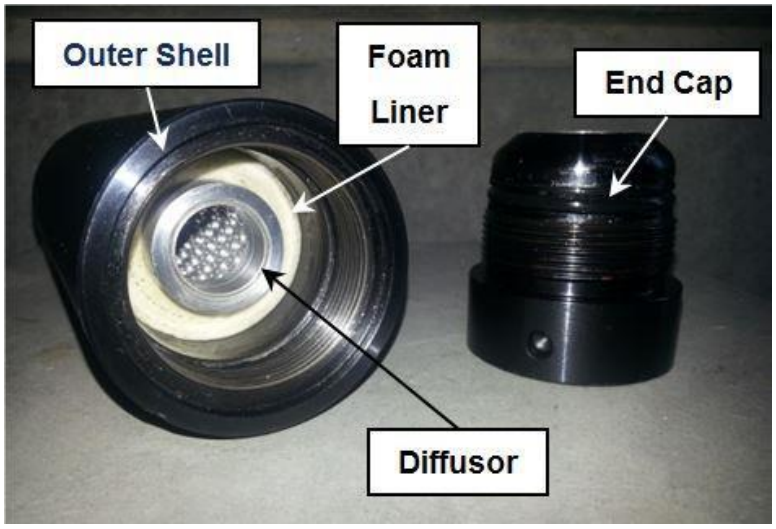

Figure 5 - Second-generation of liner-style suppressor [4].

1.2 Scope of the Project

A third generation of liner-style suppressors was developed that allowed for flexibility in the initial volume fraction (VF) of microspheres, the initial microsphere pressurization (IMP) of the microspheres, and the properties of the host matrix. Each component of the suppressor was considered both individually and as it would function within the system.

1.2.1 Suppressor Development

A third generation of liner-style suppressor was developed that had comparable performance to the previous iterations of foam, but allowed for more flexibility in foam material properties. The initial microsphere pressurization (IMP), the initial volume fraction (VF) of the microspheres within the foam, and the volume of foam within the suppressor were explored to determine their impact on the suppressor transmission loss (TL). The use of additives to alter the hardness and compression set of the foam were

explored to determine their impacts on the utility of the foam in terms of TL and material compatibility, which will manifest as performance changes due to repeated exposure to the hydraulic environment.

The use of a diffuser in liner-style suppressors was considered based on a review of available literature and the implications of the solid mechanics of the liner. An examination of the solid mechanics of the liner implies that it is generally not preferable to use a diffuser with syntactic liners. For this reason, diffusers were not used in the third-generation suppressors, and will not be used in future generations.

1.2.2 Testing

Third-generation suppressors were transmission loss tested according to ISO 15086. The form factor of the diffuser shell and the geometry of the liners were kept constant so that only the composition of the liner was varied. The frequency range considered was 0 to 4000 Hz, as the majority of the energy contained by the fluid-borne noise in hydraulic systems is below 1000 Hz. Each liner-style suppressor was tested over a range of system pressures from 1.38 to 13.8 MPa to characterize its effectiveness as a noise treatment device. Each liner was then tested an additional two times to determine whether or not the foam was damaged by the hydraulic environment.

1.3 Overview of Thesis

The following chapters will outline the background of the work, the design considerations of acoustic diffusers in in-line suppressors, and the design of the syntactic foam in terms of composition. Chapter 2 provides background information about acoustic

noise control in general, compliant-style suppressors, and syntactic foam. Chapter 3 reviews the use of a diffuser in bladder-style and liner-style suppressors. Chapter 4 discusses the composition of the liner in greater detail and the test articles used to demonstrate the influence the foam components in the acoustic performance of the suppressor. Chapter 5 provides experimental method and data that demonstrates the contributions of alterations that were made to the composition of the foam. Conclusions are drawn from the experimental results and design considerations in Chapter 6. Supplemental material related to various topics discussed in this paper can be found in the appendices.

CHAPTER 2. BACKGROUND

Noise sources in the hydraulic environment will be discussed first, then the physical principles by which noise is controlled in hydraulic environments will be discussed. Several resonance-style devices will be described that use resonance to control fluid-borne noise. Compliance-style, inline suppressors are discussed along with an introduction to bulk modulus a material property. The relationship between the acoustic impedance and bulk modulus will be introduced as it relates to the acoustic performance of suppressors. Syntactic foams and the composition of the liners are introduced along with component properties that will be important to the functioning of liner-style suppressors.

2.1 Hydraulic Noise Sources

Most of the acoustic energy in hydraulic systems is generated by the pumps, which produce strong tones at the pump's passing frequency and its harmonics. Due to the typical designs of hydraulic pumps, the pump passing frequency and the first several harmonics are below 1000 Hz. Orifices and other flow path geometries will introduce broadband noise which will generally have a lower magnitude – but not insignificant – than the pump tones. Consequently, most of the acoustic energy in a hydraulic system will have a frequency less than 1000 Hz.

Reduction of noise generation is not usually emphasized when designing hydraulic pumps and system components as other functionalities are more highly prioritized by the hydraulics industry. Therefore, the most common method by which the

fluid-borne noise of hydraulic systems can be mitigated is through the addition of noise control devices.

2.2 Hydraulic Noise Control

In general, two varieties of hydraulic noise control devices exist; resonant-style and compliant style devices. Both varieties of hydraulic noise control devices create a specific acoustic impedance mismatch within the hydraulic circuit which reduces the acoustic energy that is transmitted past the mismatch.

2.2.1 Resonant-Style Noise Control Devices

Resonant-style devices usually incorporate a side branch to the hydraulic circuit in which resonances are excited. Typical resonator devices include ¼ and ½ wave resonators and Helmholtz resonators. The basic functioning of ¼ and ½ wavelength resonator is the same, the side branches have one end rigidly capped and one open end which allows resonant waves to be created at multiples of the branch's fundamental frequency; odd integer multiple in the case of ¼ wave resonators and integer multiples in the case of ½ wave resonators.

The wavelength of an acoustic wave is inversely proportional to the frequency of the sound such that

$$\lambda = \frac{c}{f} \tag{2.1}$$

where c is the speed of sound in the fluid through which the sound is propagating and f is the frequency of the sound. As the speed of sound in hydraulic oil is approximately 1500

meters per second, and most frequencies of interest in hydraulic system are low – less than 1000 Hz – the corresponding wavelengths are large. For example, given SAE-40 hydraulic oil, and a frequency of 225 Hz – the pump passing frequency of a 9-piston pump operating at 1500 rpm – the wavelength is roughly 6.5 meters, thus requiring 3.25 meter or 1.63 meter side branches. Because the wavelengths of the acoustic waves being treated are large, the devices used to treat sound in hydraulic systems are often prohibitively large to be used in many hydraulic systems.

Helmholtz resonators are common noise control devices, but only effectively treat noise at or near the resonant frequency of the device. Helmholtz resonators are comprised of a cavity with a specific volume of fluid that is connected to the flow path via a neck of specific length and cross-sectional area. Altering the length of the neck, cross-sectional are of the neck, and the cavity volume will change the effectiveness of the device and the resonant frequency. For hydraulic applications, the required dimensions of Helmholtz resonators are too large to be used in mobile systems [5].

2.2.2 Compliant-Style Noise Control Devices

Changes in the cross-sectional area of the flow path or the propagation medium is used to produce the specific acoustic impedance mismatch in compliant-style devices. The simplest compliant-style noise control of device – those that rely on a change in the cross-sectional area of the flow path to create the mismatch in specific acoustic impedance – are called expansion chambers. For the hydraulics application, in which through flow of the oil is necessary, all other compliant-style devices are modifications of the expansion chamber design. Currently, the only commercially available design that

uses a change in the propagation medium to create the specific acoustic impedance mismatch are bladder-style suppressors. Liner-style suppressors have been in development, in which a foam is used to introduce compliance to the suppressor [1,4].

2.2.2.1 Bulk Modulus and Acoustic Impedance

By definition, the bulk modulus of an acoustic medium is given by

$$K = \rho_0 \left(\frac{\partial P}{\partial \rho_0} \right)_{\rho_0} \tag{2.2}$$

where P is the pressure in the medium and ρ is the density of the medium. An examination of Equation (2.2) implies that the bulk modulus is constant across all frequencies. Additionally, increasing the bulk modulus of the medium is an equivalent statement to decreasing the compliance of the medium.

The specific acoustic impedance in a waveguide, such as a pipe, is related to the bulk modulus by

$$Z = \frac{\sqrt{\rho K}}{A} \tag{2.3}$$

where A is the cross-sectional area of the waveguide and ρ is the density of the medium. An examination of Equation (2.3) implies that decreasing the bulk modulus of the medium will decrease the acoustic impedance.

In most hydraulic applications, the specific acoustic impedance of the system is prescribed by the volumetric flow rate and system pressure. Inline suppressors create a disparity in the specific acoustic impedance by increasing the cross-sectional area or by reducing the bulk modulus in the suppressor or both. While decreasing the cross-sectional

area or increasing the bulk modulus may be possible, the performance restrictions in hydraulic systems make these routes impractical.

2.2.2.2 Expansion Chamber

The transmission loss of an expansion chamber is only dependent on the geometry of the chamber and the geometry of the inlet and outlet ports of the chamber. As the ratio of the cross-sectional area of the chamber to the cross-sectional area of the inlet and outlet ports is increased, the peak transmission loss will increase. Expansion chambers are frequency dependent devices, with the transmission loss increasing to a peak and reducing to a null in a periodic manner in frequency that is related to the length of the expansion chamber.

2.2.2.3 Bladder-Style Suppressors

Bladder-style suppressors are a modification on the expansion chamber design, in which sound is allowed to propagate into a gaseous medium, usually nitrogen, which is restrained in the suppressor by use of a flexible rubber bladder. The gas is substantially less stiff than the hydraulic oil, creating a large mismatch in the specific acoustic impedance. Using the perfect gas law and examining Equation (2.2), it can be shown that the Bulk modulus of a gas is the pressure of the gas. In the case of bladder-style suppressors, and above the charge pressure, the pressure of the gas is the system pressure. Thus, the effectiveness of these devices is sensitive to the pressure of the gas in the suppressor, with peak effectiveness at approximately 90% of the system operating pressure [1].

Of the commercially available noise control devices for hydraulic systems bladder-style suppressors are the most effective devices for treating broadband noise. As bladder-style suppressors rely on many of the same physical phenomena as liner-style suppressors, the bladder-style suppressors will be discussed in greater detail in Chapter 3.

2.2.2.4 Liner-Style Suppressors

Liner-style suppressors use a solid medium – in this case, syntactic foam – by which compliance is introduced to the suppressor. The syntactic foams used for this application are comprised of a polymer host matrix and a polymer microsphere. The main function of the host matrix is to contain the microspheres and to withstand the hydraulic environment. The microspheres are filled with gas, usually nitrogen, and are the main source of compliance in liner-style devices.

2.3 Syntactic Foam

Compliance is introduced in liner-style suppressors by means of a syntactic foam liner. The mechanical and acoustic properties of the liner will be controlled by the properties of the liner's two constituent components; i.e. the microspheres and the host matrix. The bulk modulus of the syntactic foams will be the means through which compliance is discussed in this thesis as it is useful to have a single value to characterize a foam and most solid mechanics material modelling is done in terms of bulk modulus.

2.3.1 Microspheres

The liner will have two regimes of behavior that will be determined by the solid mechanics of the microspheres, which are essentially thin-walled pressure vessels [6]. At

atmospheric pressure, and relatively low external pressures, the microspheres behave similarly to rigid spheres. At elevated external pressures, the walls of the microsphere will collapse, a condition referred to as buckling. After the microspheres have buckled, they will behave like bubbles within the liner. The critical pressure at which the microsphere will buckle can be found as

$$P_{cr} = P_{ext} - P_{\text{int}} = \frac{2Et_w^2}{r_w^2\sqrt{3\left(1-\nu^2\right)}} \tag{2.1}$$

where P_{ext} is the exterior pressure, P_{int} is the interior pressure, E is the Young's modulus of the microsphere, t_w is the wall thickness of the microsphere, r_w is the radius of the microsphere, and ν is the Poisson's ratio of the microsphere. The critical pressure is a differential pressure across the wall of the microsphere, above which the microsphere will buckle. From the critical pressure, the system pressure at which the microspheres will collapse can be found as

$$P_{collapse} = IMP + P_{cr} \tag{2.2}$$

where *IMP* is the initial microsphere pressurization. Below the collapse pressure of the microspheres, the foam will be inefficient at treating noise when compared to foam in the post collapse regime. Gruber [1] showed that it is theoretically beneficial for the treatment of noise in hydraulic systems to drive the collapse pressure toward the system operating pressure. Micrographs of pre-collapsed and post-collapsed microspheres can be seen in Figure 6.

a) b)

Figure 6 – Micrograph of microspheres in the a) pre-collapsed and b) post-collapsed state [7].

The limit of the IMP is the burst pressure, which can be found as

$$P_{burst} = P_{\text{int}} - P_{ext} = \frac{2t_w \sigma_{yield}}{r_w} \tag{2.3}$$

where σ_{yield} is the yield stress of the microsphere. The burst pressure is a differential pressure above which the microsphere will rupture and release the internal pressure. After a microsphere has burst, it will not act as an effective noise treatment, hence the burst pressure is the upper limit of the IMP that the microspheres can sustain if handled at atmospheric pressure.

2.3.2 Host Matrix

The host matrix selection is critical to the functioning of the liner, as it will affect the acoustic properties over all pressure ranges. Because the microspheres must be mixed into the host matrix prior to the host matrix solidifying, two part polymers are used.

The host matrix of the syntactic foams used for first- and second-generation hydraulic suppressors used a polyester polyurethane fabricated by UTC Aerospace Systems. The chemical composition of the polyurethane in previous generations of suppressors was fixed, with only the geometric form of the liner being available for design by researchers. This lack of compositional flexibility limited the development of the liner-style devices.

CHAPTER 3. DIFFUSER DESIGN CONSIDERATIONS

The diffuser in a hydraulic suppressor serves both an acoustic and a structural purpose in the suppressor. The acoustic purpose of the diffuser is to introduce acoustic resistance, and thus reduce the transmitted fluid-borne noise. Structurally, the diffuser is used to restrain and locate the bladder or liner in the suppressor. To effectively meet both the acoustic and structural demands, the diffuser is usually composed of two parts, as is shown in Figure 7. The main body bears most of the structural loading applied by the bladder or liner, while the perforate sheet provides most of the acoustic resistance through viscous effects. The perforate sheet generally sheathes the main body, both limiting the potential of bladder or liner extrusion through the holes in the main body and providing the majority of the acoustic resistance.

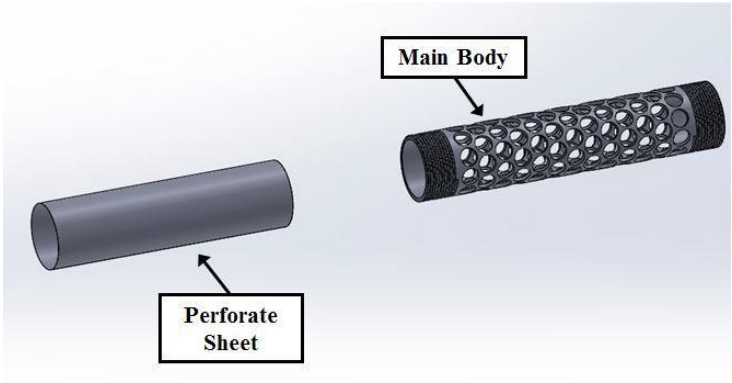

Figure 7 – Exploded view of a typical design for a diffuser [4].

3.1 Basic Theory of Diffusers

Diffusers add damping to the suppressor via viscous drag in which the energy loss is proportional to the acoustic particle velocity. This damping will tend to decrease the maximum achievable transmission loss, but increase the minimum transmission loss which can broaden the frequency range over which the suppressor is useful as a noise

treatment device. The effectiveness of a diffuser as a noise control device will increase with increased acoustic particle velocity. The acoustic particle velocity can be calculated as

$$u = \frac{p}{Z_0} \tag{3.1}$$

where p is the acoustic pressure, and Z_0 is the specific acoustic impedance. As in-line hydraulic suppressors reduce the specific acoustic impedance within the suppressor this will result in an increased acoustic particle velocity and an increased effectiveness of the diffuser.

3.1.1 Acoustic Impedance Modelling

Salmon [4] discussed the development and implementation of an impedance model of the main body and perforate sheet that can be used to predict the acoustic performance of the diffuser. The model discussed is based on the assumption that the medium on either side of the diffuser has identical impedance. The acoustic impedance is dependent on diffuser, system, and acoustic parameters.

3.1.2 Structural Requirements

Diffusers can be treated similarly to thin shelled pressure vessels, with forces acting upon them due to fluid flow through the diffuser and contact with the bladder or liner [4]. At steady state, the static fluid pressure differential between the sides of the diffuser will be zero; however, due to viscous effects, the acoustic pressure differential will not be zero. Diffusers that are not designed to bear these loads may fail which can lead to contamination of the hydraulic system.

3.2 Applicability to Bladder-Style Suppressors

For the case of a bladder-style suppressor, the use of a diffuser is necessary structurally and can be beneficial acoustically. The diffuser serves a critical structural role when used in a bladder-style suppressor, as the diffuser prevents the bladder from becoming disconnected from the shell of the suppressor and traveling freely through the hydraulic system. A failure of the diffuser could create many additional problems in a hydraulic system such as increased risk of cavitation by introducing nitrogen to the oil and valve failure or dead heading from the bladder becoming lodged in the system. Dead heading is a term of art that refers to a condition in which there is now flow path through the hydraulic system, thus causing a large spike in pressure in constant flow pumps.

The thickness of the viscous boundary layer is given by

$$t_v = \sqrt{\frac{2\mu}{\rho\omega}} \tag{3.1}$$

where μ is the fluid viscosity, ρ is the density of the fluid, and ω is the angular frequency of the dynamic pressure [8]. If the radius of the holes in the perforate sheet are less than or equal to the thickness of the viscous boundary layer, then acoustic communication may not exist across them [8]. For SAE 40 oil at 20° C holes with diameters less than 1.6 mm may not allow acoustic communication of frequencies lower than 250 Hz., if the perforate sheet is thick. As most acoustic energy in hydraulic systems is contained below 1000 Hz, this may be significant to the overall performance of the diffuser.

3.3 Applicability to Liner-Style Suppressors

In a liner-style suppressor a liner will experience a hydrostatic loading when used, which may result in a degradation of the diffuser's acoustic performance. Additionally, the material composition of the liner can lead to compression setting (permanent dimensional changes resulting from a compressive load), which will also impact the suitability of diffusers in liner-style suppressors.

3.3.1 Solid Mechanics of Liners

Liners are annular cylinders, as shown in Figure 8. Because the liner is not adhered to the walls of the suppressor, the liner will undergo hydrostatic loading at the system pressure. This geometry of foam allows for the liner to sheath the diffuser, and allows the oil to have an unimpeded flow path through the suppressor. The critical dimension of the liner for use with a diffuser is the inner radius; under hydrostatic loading, the change in the inner radius can be calculated as

$$\Delta r_i = \frac{P_{sys} r_{i,1}}{E^*} \left(\frac{r_{i,1}^2 \left(1+\nu^*\right) - r_{o,1}^2}{r_{o,1}^2 - r_{i,1}^2} \right) \tag{3.2}$$

where $r_{o,1}$, and $r_{i,1}$, are the initial inner and outer radii of the liner, as defined in Figure 8, E^* is the effective Young's modulus of the foam, ν^* is the effective Poisson's ratio of the foam, and P_{sys} is the system pressure [9]. It should be noted that the effective Young's modulus and the effective Poisson's ratio will change with the system pressure, as discussed in Section 4.1. An examination of Equation (3.2) indicates that increasing the hydrostatic pressure will result in a decrease in the inner radius of the liner if

$$\frac{r_{o,1}}{r_{i,1}} > \sqrt{1+\nu^*} \tag{3.3}$$

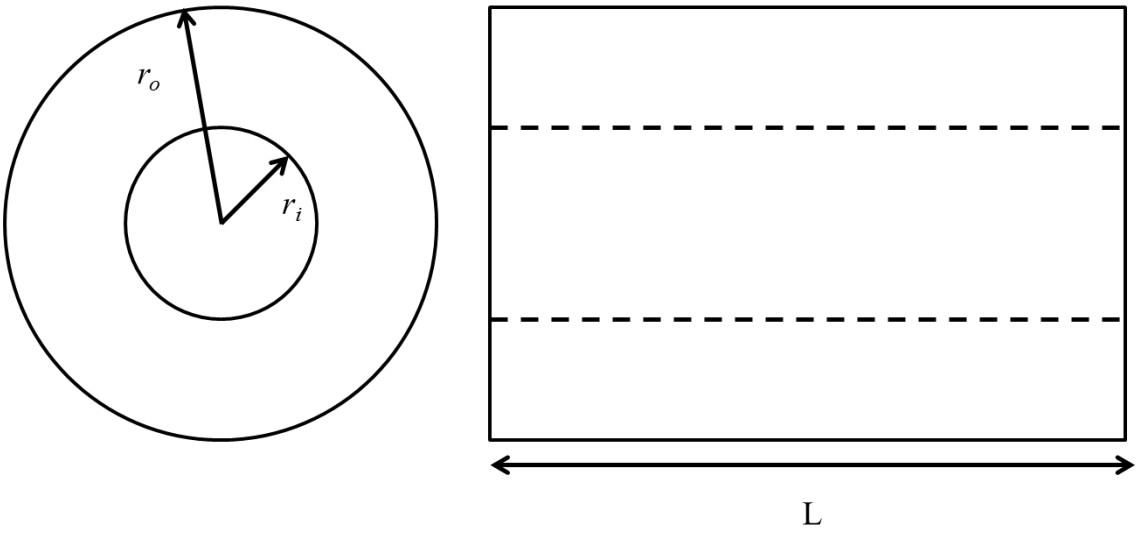

Figure 8 – Annular cylinder of syntactic foam. Reference dimensions for equations (3.2) and (3.3).

The decrease in the inner radius of the liner can cause the liner to come into contact with the outer radius of the diffuser at elevated system pressures. Liners are typically designed to have the maximum volume and are therefore installed with the inner radius in contact with the diffuser, narrowing the pressure range over which the liner may not be in contact with the diffuser. Additionally, this will increase the loading experienced by the diffuser and violate the assumptions used to model the acoustic behavior of the diffuser. The loading on the diffuser will cause significant stresses in both the perforate sheet and the liner, potentially resulting in a failure of one or both components.

Contact between the diffuser and the liner will also impact the acoustic characteristics of the diffuser. The assumption of a continuous medium on either side of

the diffuser is violated, so the analysis of performed by Salmon will not be valid. While the exact modeling of the acoustic characteristics of the diffuser has not been undertaken, it is known that the diffuser can decrease the acoustic performance of a liner style suppressor [4]. The data presented in Figure 9 was gathered using identical liners at the same system pressure, with the only difference being the addition of the diffuser. The liner with diffuser has a significantly lower transmission loss in the range of 100 to 1250 Hz, which is the range in which most acoustic energy in hydraulic systems exists.

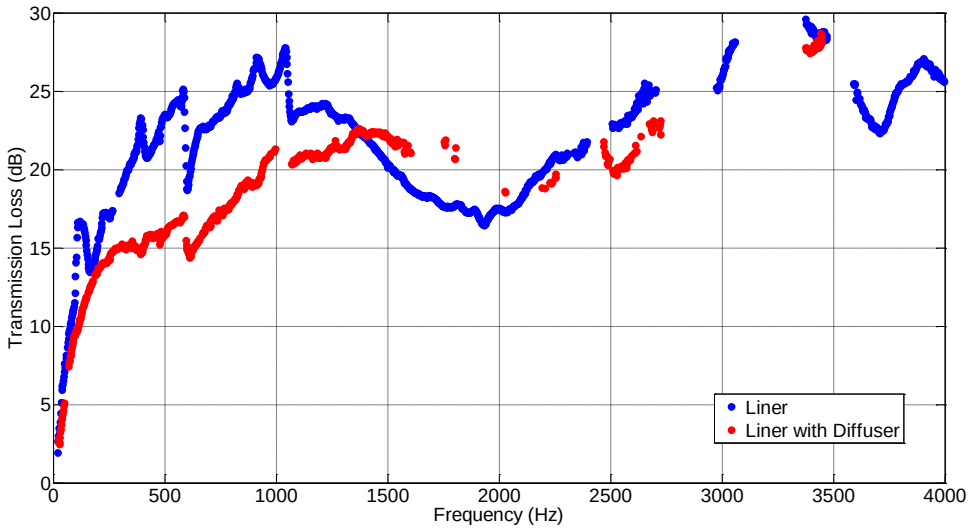

Figure 9 – Impact of the use of a diffuser in a liner-style suppressor [4].

While it may be possible to design the liner to not come into contact with the diffuser by altering either the initial dimensions or the material properties of the foam, this may negatively impact the effectiveness of the suppressor. The required dimensional changes would decrease the initial volume of foam and result in decreased compliance in the suppressor, decreasing the transmission loss.

3.3.2 Compression Sets

Most polymer based syntactic foams will have a permanent shape change when exposed to elevated temperatures and pressures for extended periods of times. The extent of these permanent shape changes, often called compression sets, will depend on both the composition of the polymer, and the curing processes of the polymer. The permanent set can be large enough to cause the liner to violate the diffuser assumptions even at low system pressures and to apply a static load to the diffuser.

3.3.3 Use of Diffusers in Liner-Style Suppressors

As stated in Section 3.3.1, the solid mechanics of annular cylinders indicates that the acoustic effectiveness and the structural integrity of the both the diffuser and the liner can become compromised when the liner is exposed to hydrostatic loading. Any compression set taken by the liner will only tend to increase the likelihood that the liner will come into contact with diffuser and compromise the acoustic effectiveness of the device and the structural integrity of the diffuser and liner. These considerations make it ill-advisable to use a diffuser in a liner-style suppressor.

CHAPTER 4. INFLUENCE OF CONSITUENT PROPERTIES ON THE SYNTACTIC LINER

This chapter discusses the bulk modulus modelling of a syntactic foam and then discusses the influence of the initial volume fraction on the bulk modulus and the test articles used to explore alterations in the initial volume fraction independently of other factors. The influence of the initial microsphere pressurization on the syntactic foam is then discussed along with the test articles used to experimentally explore the influence of the initial microsphere pressurization independently of other factors. Material properties that influence the material compatibility of both the microspheres and host matrices are then discussed. Polymer additives that can influence the material compatibility of the host matrix are discussed along with the test articles used to explore the influence of those additives independently of other factors. Modelling of the volume of the foam within the suppressor is then discussed.

4.1 Composite Properties

The foam is used to create a mismatch in the specific acoustic impedance between the suppressor and the rest of the hydraulic system, which will cause a portion of the incident acoustic energy to be reflected towards its source. It is well known that the greater the disparity between the specific acoustic impedances, the more effective the noise treatment. As previously stated, the specific acoustic impedance is directly related to the square root of the bulk modulus of the acoustic medium.

Hashin [10] showed that the bulk modulus of a composite such as a syntactic foam can be calculated as

$$K^* = K_u + (K_v - K_u)\frac{(4G_u + 3K_u)F_v}{4G_u + 3K_v + 3(K_u - K_v)F_v} \tag{4.1}$$

where K is the bulk modulus, G is the shear modulus, F_v is the volume fraction of the voids, and the subscripts u and v refer to the urethane and void, respectively.

The bulk modulus of a syntactic foam is a function of the effective Young's modulus and the effective Poisson's ratio such that

$$K^* = \frac{E^*}{3(1-2\nu^*)} \tag{4.2}$$

where E^* and ν^* are the effective Young's modulus and the effective Poisson's ratio, respectively [9]. Thus, in the pre-collapse regime where the composite bulk modulus is constant, the effective Young's modulus and the Poisson's ratio will remain constant. Similarly, in the post collapse regime, where the composite bulk modulus varies, the effective Young's modulus and Poisson's ratio will vary.

4.1.1 Influence of Initial Volume Fraction

At any given pressure the volume fraction of the of microspheres in a syntactic foam, F_v is given by

$$F_v = \frac{V_{\mu S}}{V_u + V_{\mu S}} \tag{4.3}$$

where $V_{\mu S}$ and V_u are the volumes of the microspheres and urethane, respectively. The microspheres in the foam can be treated as thin-walled pressure vessels and will buckle, or collapse, when the differential pressure across the wall of the microsphere exceeds the collapse pressure. At this point, the voids will become significantly less rigid and can be treated as gas pockets embedded in the syntactic foam [6]. Equations (4.1) and (4.3)

imply that the volume fraction of the microspheres in the syntactic foam should be maximized at any given pressure to decrease the bulk modulus of the syntactic foam.

Prior to buckling, F_v and K_v are roughly constant; consequently, the bulk modulus of the syntactic foam will remain constant. Further, the syntactic foam is at its most rigid state in the pre-collapse regime, and will therefore be at its least effective state for noise treatment. In the post-collapse regime, the buckled microspheres will act as bubbles, or voids, within the syntactic foam. In the post-collapse regime, the volume occupied by the microspheres is given by

$$V_{\mu S}\left(P_{sys}\right) = \frac{IMP}{P_{sys}} \times VF \tag{4.4}$$

where *VF* is the initial volume fraction, *IMP* is the initial microsphere pressurization, and P_{sys} is the system pressure. The bulk modulus of the voids in the post-collapse regime can be calculated as

$$K_v\left(P_{sys}\right) = \rho_v \frac{\partial P_v}{\partial \rho_v} = P_{sys} \tag{4.5}$$

where ρ_v and P_v are the density and pressure of the gas in the voids, respectively.

4.1.2 Initial Volume Fraction Test Articles

The impacts of increasing initial volume fraction on the acoustic performance of third-generation liner-style suppressors were explored experimentally through transmission loss testing, using the test articles listed in Table 3. To eliminate any confounding variables, the liners listed in Table 3 were fabricated with the same composition of host matrix, and the same dimensions. An explanation of the naming

convention used for the test articles can be found in APPENDIX A. Polymer Composition.

Table 2 – Initial Volume Fraction Test Articles

Test Article	IMP [MPa]	VF [%]	IMP [psig]
VT-0-0-1-50-0-N-L	0	50	0
VT-0-0-1-40-0-N-L	0	40	0

4.1.3 Influence of Initial Microsphere Pressurization

In addition to the implications on initial volume fraction, Equation (4.4) implies that maximizing the IMP will result in the maximum volume fraction of the voids at any given pressure, thus decreasing the bulk modulus of the syntactic foam at any pressure.

4.1.4 Initial Microsphere Pressurization Test Articles

The impacts of increasing IMP on the acoustic performance of third-generation liner-style suppressors were explored experimentally through transmission loss testing, using the test articles listed in Table 3. To eliminate any confounding variables, the liners listed in Table 3 were fabricated with the same composition of host matrix and same the same dimensions.

Table 3 – Initial Microsphere Pressurization Test Articles

Test Article	IMP [MPa]	VF [%]	IMP [psig]
VT-0-0-1-50-0-N-L	0	50	0
VT-0-0-1-50-20-N-L	0.138	50	20
VT-0-0-1-50-50-N-L	0.345	50	50

There is reason to suspect that the 0.138 MPa (20 psig) IMP liner was not charged to 0.138 MPa, but rather to 0.034 MPa (5 psig) due to an uncalibrated differential pressure gage that was used in the charging apparatus. The miscalibration was noticed on

the following use, where the gage atmospheric pressure was measured as 0.103 MPa (15 psig) rather than 0 MPa as should have been measured.

4.1.5 Influence of Liner Bulk Modulus on the Bulk Modulus in the Suppressor

The bulk modulus in the suppressor can be determined by adding the bulk moduli of the liner and oil like springs in parallel, with corrections made for the volume of each component. The bulk modulus in the suppressor can be calculated as

$$K_{\text{sup}} = \left(\frac{V_{oil} / V_{cav}}{K_{oil}} + \frac{V_{foam} / V_{cav}}{K^*} \right)^{-1} \tag{4.6}$$

where V_{oil} is the volume of oil within the suppressor, V_{cav} is the volume of the suppressor, V_{foam} is the volume of the syntactic foam liner in the suppressor, and K_{oil} is the bulk modulus of the hydraulic oil. An examination of Equation (4.6) implies that increasing the volume of the liner will decrease the bulk modulus of the suppressor, thus increasing the effectiveness of the suppressor, if the bulk modulus of the liner is less than that of the oil.

4.2 Microsphere Material Properties

The volume and pressure of the gas in the liner are critical features of the liner, as these quantities govern the bulk modulus of the liner at elevated pressures. The microspheres are the means by which gas is introduced to the liner, so the physical properties of these spheres are of great importance to the functioning of the liner.

The Young's modulus, Poisson's ratio, yield stress, and the glass transition temperature (T_g) are the critical properties of the microsphere materials. The Young's

modulus, Poisson's ratio, and yield stress of the microspheres along with the microsphere's dimension govern the collapse and burst pressure of the microspheres. Above T_g, the material properties of the microspheres will change drastically, becoming brittle and incapable of holding gas. As it is critical that the microspheres hold gas, T_g acts as an upper limit to the local temperature in the liner during processing and curing.

4.3 Host Matrix Material Properties

The host matrix selection is critical to the functioning of the liner both above and below the buckling pressure of the microspheres. In the region below the buckling pressure the bulk modulus of the liner is dominated by the bulk modulus of the host matrix. In the region above the buckling pressure, the bulk modulus of the host matrix will be the upper bound limit of the bulk modulus of the liner. It has been shown that minimizing the Young's modulus and maximizing the Poisson's ratio of the host material will result in an acoustically superior liner [1].

4.3.1 Material Compatibility

Two-part polymers were considered for the host matrix of the liner to allow the microspheres to be added, thus creating a syntactic foam. Most two-part polymers fall into two classes: silicone rubbers and polyurethane rubbers. Silicone rubbers typically do not have good resistance to petroleum and hydraulic oils, making them ill-suited as a candidate for the host matrix. Additionally, it is known that polyester-based polyurethanes are better suited to the hydraulic environment than polyether-based polyurethanes.

The host matrix of the liner must be compatible with both the microspheres that will be embedded within it and the hydraulic environment. Damage to the microspheres will result in the release of gas, which will increase the bulk modulus of the liner and, correspondingly, decrease the effectiveness of the liner as a noise treatment device. The hydraulic environment is severe, with temperatures ranging from -40° C to 200° C, pressure ranges from 1.4 to 42 MPa, and potentially reactive chemicals.

The microsphere glass transition temperature, T_g, acts as an upper limit to local temperature in the liner during processing and curing. It is known that the polyurethane reaction is exothermic, which will increase the temperature within the liner above the curing temperature. For the microspheres used in the third-generation liner-style suppressors, the transition temperature is approximately 80° C; to stay below this limit, a host matrix was selected to be processed and cured at 60° C.

4.3.2 Component Properties

Polyurethanes are generally two-part polymers, in which an isocyanate is reacted with a polyol. The isocyanate and polyol sides of the host matrix must not be too viscous for the microspheres to be mixed into them. There are two general alternatives to lowering the viscosity of the isocyanate or polyol side of the polyurethane: increasing the mixing temperature, or using additives. Increasing the temperature of a side of the polymer generally allows the prepolymer molecules to slide past one another more easily; however, the handling temperature of the prepolymers is limited by the T_g of the microspheres.

4.3.3 Influence of Material Additives

The methylene diphenyl diisocyanate (MDI) polyether polyurethane used in the third-generation liner-style suppressors is a two-part polymer, in which a mixture of chemicals containing isocyanate bonded to some polymer chain is reacted with a mixture of chemicals containing polyols that are bonded to some polymer chain. These two mixtures of chemicals are generally referred to as sides of the polyurethane reaction.

A variety of additives can be used to change the viscosity of the sides of the polymer and/or to alter the final material properties of the foam. Those additives that participate in the polyurethane reaction are called reactive additives, and those additives that do not participate in the polyurethane reaction are referred non-reactive additives. Reactive additives will change the properties of the liner and must be considered when calculating the mass ratio of the isocyanate side to the polyol side, see Appendix B. Small quantities of additives that will not alter the polyurethane reaction, such as a surfactant, can be used to decrease both the viscosity and the surface tension of a side. Decreasing the viscosity of a side of the polyurethane will increase the volume fraction of microspheres that can be mixed into that side, increasing the achievable initial volume fraction of microspheres. Decreasing the surface tension of the side will increase the ease of pouring and degassing the side, increasing the fidelity of the liner and the consistency of the material properties.

One reactive additive increased bulk modulus of the host matrix but decreased the viscosity of the isocyanate side of the polyurethane. Another reactive additive was used in the polyol side of the polyurethane to increase the shear modulus of the host matrix

which is thought to be critical for the material compatibility of the liner. A non-reactive additive was used that significantly decreased the viscosity of the isocyanate side without impacting the final properties of the foam.

The specific chemicals used to create the host matrix and the microspheres used to create the foams are listed in Appendix A, while the processing methods used to fabricate the foams are described in Appendix B.

4.3.4 Material Additive Test Articles

The impacts of the additives on the noise treatment properties of the foam were explored experimentally, using the test articles listed in Table 4. To eliminate any confounding variables, all of the foams listed in Table 4 were fabricated with 50% VF and no IMP. Test articles VT-5-0-1-50-0-N-L and VT-10-0-1-50-0-N-L have varied levels of the reactive additive in the isocyanate side of the host matrix. Test articles VT-0-1-1-50-0-N-L and VT-0-2-1-50-0-N-L have varied levels of the reactive additive in the polyol side of the host matrix.

Table 4 – Host Material Composition Test Articles

Test Article	Weight Percent of Additive in A	Weight Percent of Additive in B
VT-0-0-1-50-0-N-L	0	0
VT-5-0-1-50-0-N-L	5	0
VT-10-0-1-50-0-N-L	10	0
VT-0-1-1-50-0-N-L	0	1
VT-0-2-1-50-0-N-L	0	2

4.4 Volume of Foam

If the bulk modulus of the liner is lower than the bulk modulus of the oil, then Equation (4.6) implies that the increasing the volume of foam decreases the suppressor bulk modulus, thereby increasing the acoustic performance of the suppressor. For the liner-style of suppressor, the volume of the liner at a given pressure can be calculated as

$$V\left(P_{sys}\right)=\pi\left(L\left(P_{sys}\right)\right)\left(r_o^2\left(P_{sys}\right)-r_i^2\left(P_{sys}\right)\right) \tag{4.7}$$

where L, r_o, and r_i are defined in Figure 8, and are functions of P_{sys}. The length of the liner under a given hydrostatic load can be calculated as

$$L\left(P_{sys}\right)=L_1\left(1-\frac{P_{sys}}{E^*}\left(\frac{2\nu^* r_{i,1}^2+r_{o,1}^2\left(1-2\nu^*\right)}{r_{o,1}^2-r_{i,1}^2}\right)\right) \tag{4.8}$$

where E^* is the effective Young's modulus of the liner, ν^* is the Poisson's ratio of the liner, L_1 is the initial length of the liner, $r_{o,1}$ is the initial outer radius of the liner, and $r_{i,1}$ is the initial inner radius of the liner [9]. The outer radius of the of the liner under hydrostatic load can be calculated as

$$r_o\left(P_{sys}\right)=r_{o,1}\left(1+\frac{P_{sys}}{E^*}\left(\frac{r_{o,1}^2\left(2\nu^*-1\right)+r_{i,1}^2\left(1-\nu^*\right)}{r_{o,1}^2-r_{i,1}^2}\right)\right) \tag{4.9}$$

where all variables have been previously defined [9]. The inner radius of the of the liner under hydrostatic load can be calculated as

$$r_i\left(P_{sys}\right)=r_{i,1}\left(1+\frac{P_{sys}}{E^*}\left(\frac{r_{i,1}^2\left(1+\nu^*\right)-r_{o,1}^2}{r_{o,1}^2-r_{i,1}^2}\right)\right) \tag{4.10}$$

where all variables have been previously defined [9].

Recall that the Young's modulus and Poisson's ratio vary with system pressure which will result in changes in the volumetric behavior of the foam as the system pressure is varied.

CHAPTER 5. TRANSMISSION LOSS TESTS: METHODS AND RESULTS

This chapter will describe the type of data gathered to evaluate the acoustic performance of the third-generation liner-style suppressors that used the test articles. The conditions under which the data was gathered, and testing methodology are then discussed. Data is then presented for the third-generation liner-style suppressors that used the test articles that demonstrate the influence of initial microsphere pressurization, the influence of initial volume fraction, and the effects of additives on the material compatibility. The acoustic performance of the suppressor with the best material compatibility and acoustic performance is then compared with the acoustic performance of the first-generation liner-style suppressors.

5.1 Definition of Transmission Loss

The acoustic performance of inline suppressors is best described by the transmission loss of the suppressor. The transmission loss is generally reported in decibels, and can be calculated as

$$TL = 10\log_{10}\left|\frac{W_i}{W_t}\right| \tag{5.1}$$

where W_i is the incident acoustic energy and W_t is the transmitted acoustic energy. The insertion loss of the device was not considered to be an appropriate metric of the acoustic performance of the inline suppressors as the insertion loss is a system property rather than a property of the suppressor alone. To determine the transmission loss of the suppressor it was tested with a specialized apparatus and the data was processed in such a way that the properties of the suppressor are isolated from that of the system. The transmission loss

was evaluated for frequencies between 0 and 4000 Hz as the vast majority of acoustic energy in hydraulic systems is contained in the low frequency range, 0 to 1000 Hz.

5.2 Hydraulic Test Rig and Data Collection

The experimental apparatus and data analysis techniques used to evaluate the transmission loss of the liner-style suppressors conform to ISO-15086. A hydraulic circuit schematic of the rig is shown in Figure 10. As can be seen from Figure 10, a variable speed pump is used drive the oil through a variable orifice valve, the test section, the termination suppressor, and a loading valve. A 9-piston pump was used during testing that provided 10 gallons per minute of oil to the circuit and was driven by an alternating current motor operating at 1500 rpm. The upstream needle valve is used to induce turbulence to the hydraulic flow, thereby creating a broadband noise spectrum. The downstream loading valve was used to adjust the system pressure, and the termination suppressor was used to isolate the test section from any noise that may be produced by the loading valve.

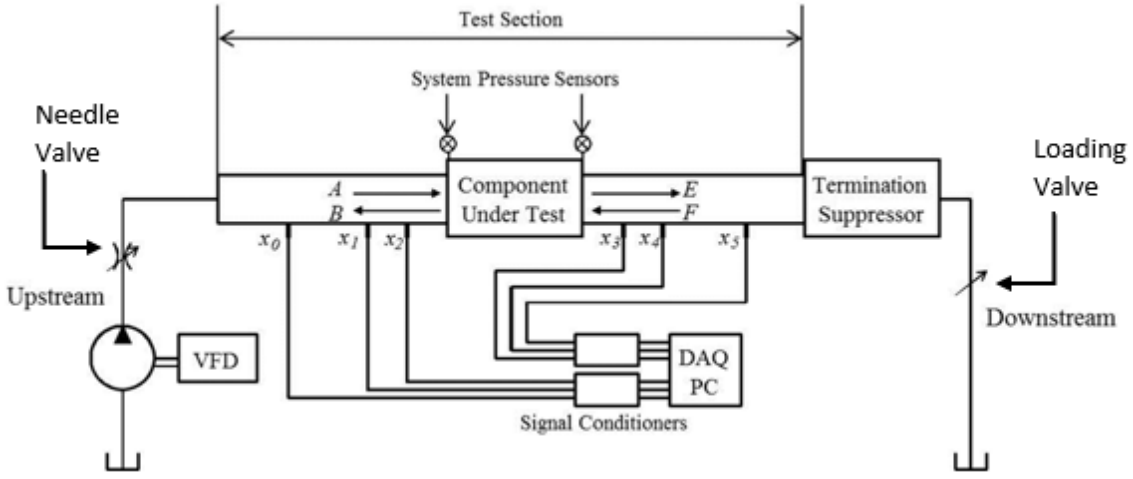

Figure 10 – Hydraulic and measurement diagram of the transmission loss measurement apparatus [4].

The test section contains two system pressure sensors, the component being tested, and the six dynamic pressure sensors necessary for accurate testing. Three dynamic pressure sensors are needed in each of the upstream and downstream portions of the test section, with unequal spacing to eliminate half-wavelength indeterminacy. Half-wavelength indeterminacy occurs when using two sensors that are located at integer multiples of half of a wavelength apart from one another [11]. The unequal spacing used is shown in Figure 11, as is prescribed by ISO-15086-2 [12].

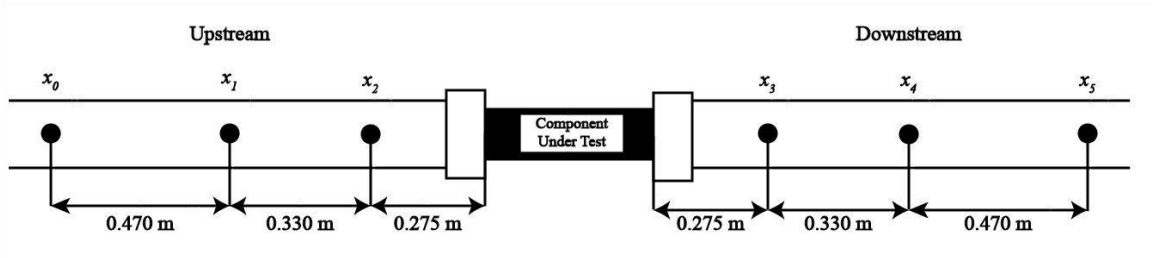

Figure 11 – Placement of dynamic pressure sensors in the test section [4].

5.2.1 Collected Data

For a given pressure, time histories are collected from all of the dynamic pressure sensors simultaneously, and the transfer functions between the signals are determined. 30 such time histories were gathered, and the transfer functions were vector averaged to form a set of composite transfer functions that are used to evaluate the transmission loss at a given pressure. Appendix C contains the code by which the collected transfer functions were processed into transmission losses. Additionally, the last set of time histories is saved to aid with communicating the results to industry sponsors; see Appendix C.2. Appendix D contains a derivation of the mathematics that drives the transmission loss processing code. The industry standard for evaluating the effectiveness

of a noise treatment device is to compare two time traces, one from the upstream section and one from the downstream section. Each time history was taken at a sampling frequency of 10800 Hz and contained a total of 5120 samples.

The noise floor, noise measured when no fluid-borne noise is present, of each of the sensors was checked every time the test rig was turned off. The noise floor is deemed acceptable if the measured signal is on the order of 40 dB lower than the signal measured when the system is turned on; this ensures that the signal to noise ratio is much greater than one. If the noise floor is deemed unacceptable, the installation of the sensor is verified, and the noise floor measurement is retaken. In addition to the noise floor, the transfer functions between the sensors are checked to ensure that the relative calibrations of the sensors have not drifted. If the relative calibration of the sensors have drifted the sensors are recalibrated before measurements are taken.

5.2.2 Sensor calibration

Imperfections in sensor manufacturing will result in variations in the dynamic responses of the sensors, which is best compensated for by regular calibration. The sensors were calibrated using the apparatus shown in Figure 12, which conforms to ISO-15086-2 [12]. This sensor calibration block is connected to the hydraulic circuit via a side branch which is installed into the test rig as the test article. Up to four transducers can be installed into the calibration block, constrained to the same axial position. As the wave field is planar in the frequency range of interest, the sensors are exposed to identical wave fields. Because the wave field each senor is exposed to is identical, the transfer functions between the sensors should be equal to 1 with a 0° phase angle between the sensors.

Using the observed transfer functions between the sensors, the transfer functions under test conditions can be adjusted to compensate for calibration discrepancies.

Figure 12 – Sensor calibration block without sensors.

5.2.3 Coherence

Coherence is a measure of the linear correlation between two sensors, and ranges in value from 0 to 1, with 0 indicating a non-linear correlation and 1 indicating a linear correlation. The coherence between sensors can be calculated as

$$C_{hi} = \frac{|G_{hi}|^2}{G_{hh}G_{ii}} \tag{5.1}$$

in post processing. G_{hj} is the cross spectral density between sensors h and i, and G_{xx} is the autospectral density of sensor x. Per ISO-15086-3 [13], if any of the seven transfer functions have a coherence less than 0.95 at a particular frequency, the data recorded at

that frequency is considered invalid and omitted from reported results. The data dropout in the transmission loss results shown in Section 5.3 is due to this coherence threshold.

5.3 Tests Performed

Each exposure to oil was comprised of a set of seven tests at different system pressures ranging from 1.37 to 13.7 MPa (200 to 2000 psig). Between 1.38 and 6.89 MPa (200 and 1000 psig, respectively) the test interval was 1.38 MPa (200 psi), as it was previously observed that the largest changes in transmission loss of liner-style suppressors occur in this range of system pressures. Between 6.89 and 13.8 MPa (1000 and 2000 psig, respectively) the test interval was broadened to 3.45 MPa (500 psi) as relatively small changes in liner-style suppressor performance occur in this range of system pressures. Tests were not run above 13.7 MPa (2000 psig) as it was observed that the performance of the liner-style suppressor were essentially constant above this system pressure.

The first set of tests performed on the liner-style suppressor was considered to be the first exposure test, and in general should have the best possible results for a foam as the effects of material compatibility should not be evident. The liner-style suppressors were installed in the test rig and data taken at consecutively higher system pressures until the maximum test pressure was reached.

The tests were repeated twice at the same system pressures to allow for statements to be made about changes in the liner-style suppressor's acoustic properties resulting from damage incurred during the testing process. Repeated tests were only performed for materials with varying amounts of additives, to determine the impacts that the additives had on the material compatibility of the liners used in the third-generation liner-style suppressors.

5.3.1 Initial Microsphere Pressurization

Figures 13 to 15 demonstrate the influence of initial microsphere pressurization on the acoustic performance of the foam. It can be seen from the figures that elevating the IMP significantly increases the transmission loss of the liner-style suppressor, thus resulting in a more effective noise control device. It can further be seen that as the system pressure increases, the advantage of the IMP diminishes, which is consistent with theory as the bulk modulus of the foam will asymptotically approach the bulk modulus of the host matrix. It can be seen from Figure 13 that at 1.37 MPa system pressure, there are clear advantages from using the 0.345 MPa IMP liner and the 0.345 MPa IMP liner in the third-generation liner-style suppressor when compared to the third-generation liner-style suppressor that used a 0 MPa IMP liner. Note that the test articles contained in these suppressors were not made with a material that was compatible with the hydraulic environment, so few conclusions can be made above 1.38 MPa.

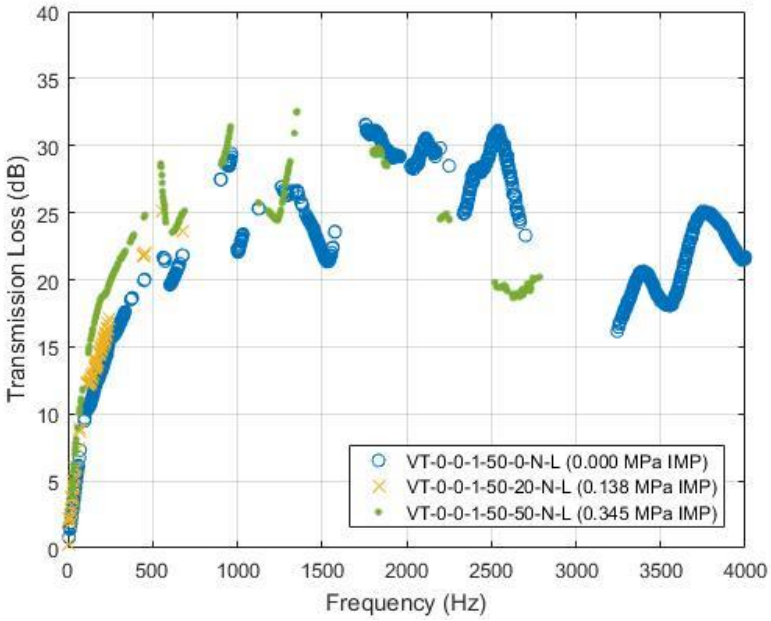

Figure 13 – Transmission loss measurements at 1.37 MPa for third-generation liner-style suppressors with liners made with varying IMP.

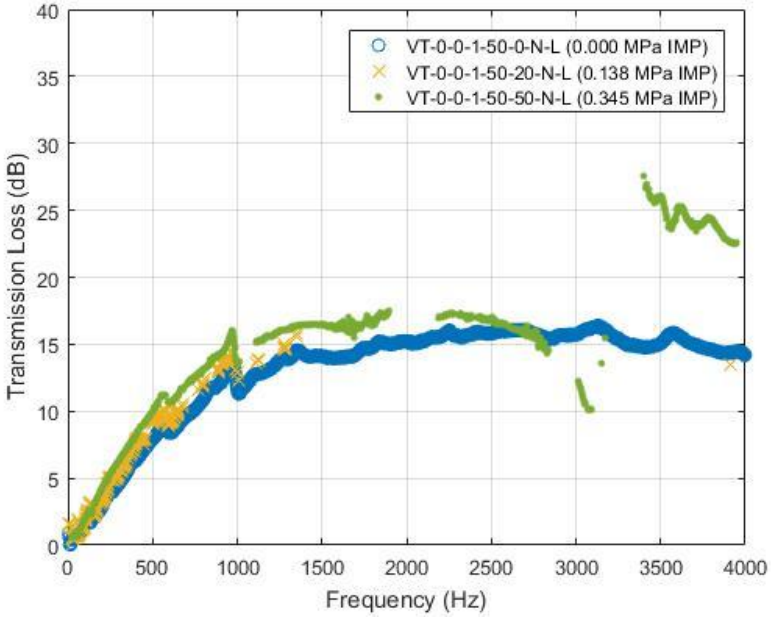

Figure 14 – Transmission loss measurements at 4.14 MPa for third-generation liner-style suppressors with liners made with varying IMP.

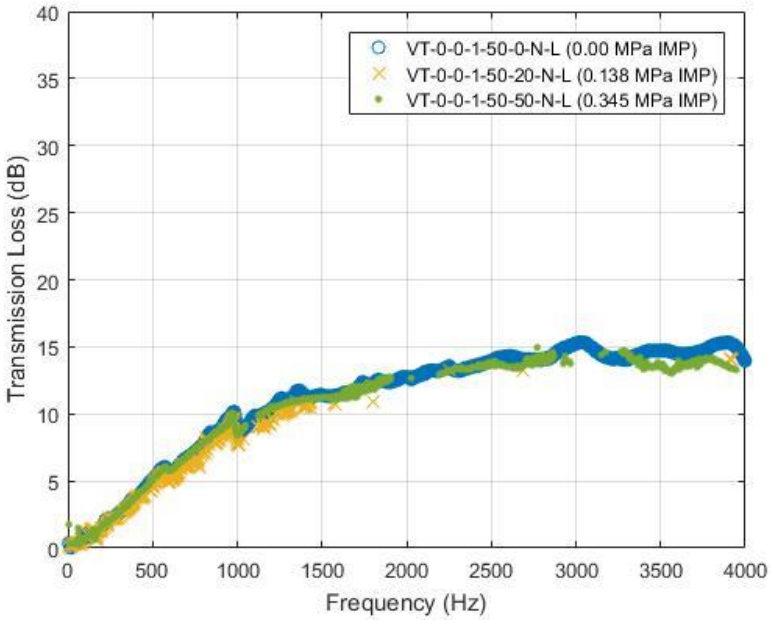

Figure 15 – Transmission loss measurements at 6.89 MPa for third-generation liner-style suppressors with liners made with varying IMP.

5.3.2 Initial Volume Fraction of Microspheres

Figures 16 to 18 demonstrate the influence of initial volume fraction of microspheres in the foam on the acoustic performance of the foam. It can be seen from the figures that increasing the VF significantly increases the effectiveness of the suppressor as a noise control device. It can further be seen that as the system pressure increases, the advantage of the increased VF persists over the system pressures of interest.

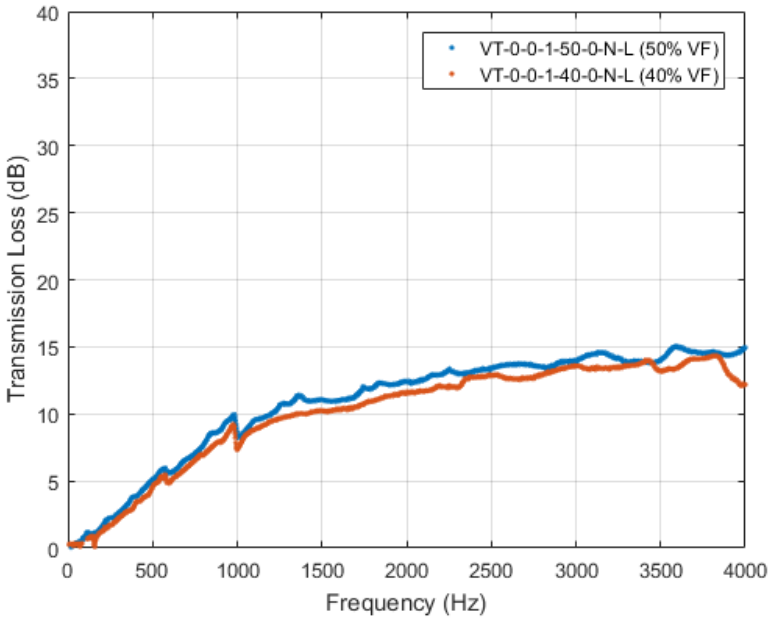

Figure 16 – Transmission loss measurements at 5.52 MPa for third-generation liner-style suppressors with liners made with varying initial volume fraction of microspheres in the liner.

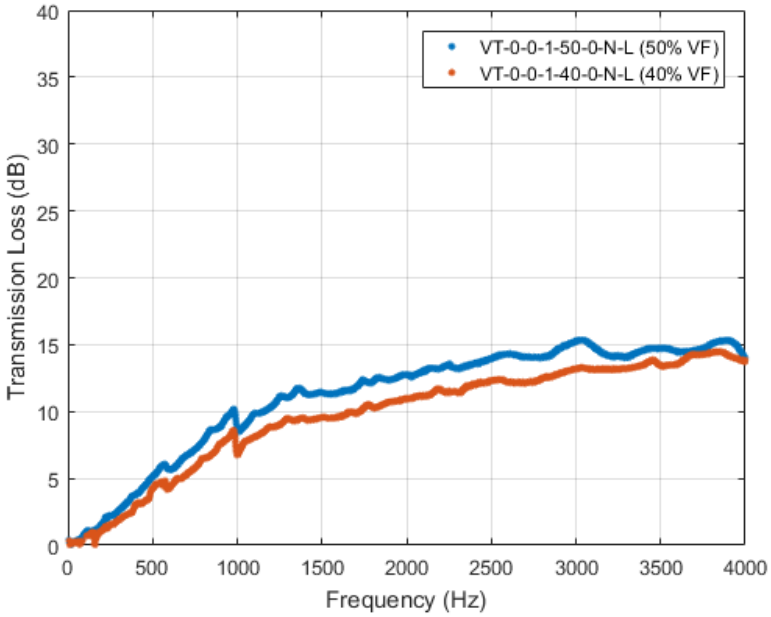

Figure 17 – Transmission loss measurements at 6.89 MPa for third-generation liner-style suppressors with liners made with varying initial volume fraction of microspheres in the liner.

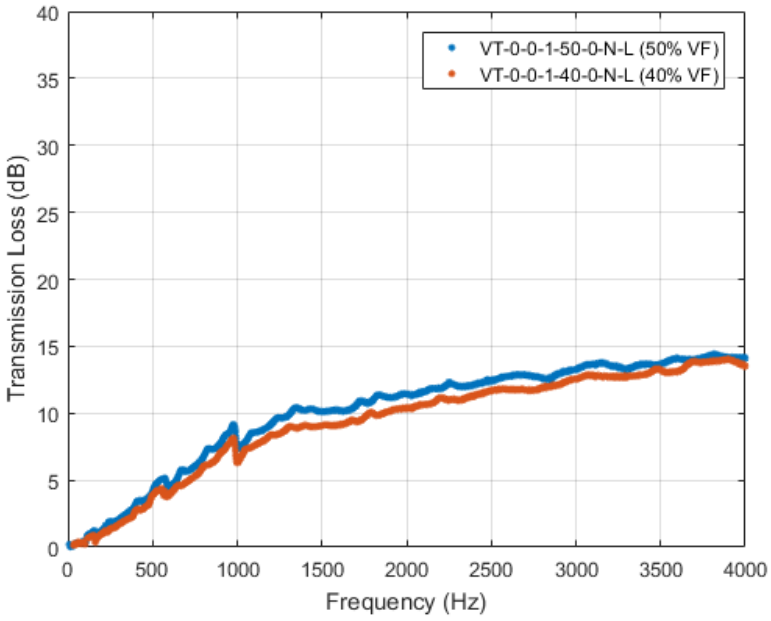

Figure 18 – Transmission loss measurements at 10.3 MPa for third-generation liner-style suppressors with liners made with varying initial volume fraction of microspheres in the liner.

5.3.3 Material Additives

The change in transmission losses were considered in each foam for successive exposures to the hydraulic environment to evaluate the ageing characteristics of each foam. The first exposure for the suppressors that used a host matrix that is compatible with the hydraulic environment, to verify that the experimental results are logical given the material modelling in Chapter 4.

5.3.3.1 Material Compatibility

Figures 19 to 23 show the results of repeated transmission loss testing at 4.14 MPA (600 psig) for third-generation liner-style suppressors that used liners with varying host matrix composition. The changes in the transmission losses depicted in Figures 19

through 23 are typical for each third-generation liner-style suppressors that used its respective host matrix composition over all pressure ranges. Any changes in the transmission losses of the suppressors over repeated tests is indicative of material property changes due to exposure to the hydraulic environment. If the material exhibits an increase in the bulk modulus then it will become less effective at treating the noise in the hydraulic system. However, if the material exhibits a decrease in the bulk modulus, seen as a broadband increase in transmission loss, the material may deform and deadhead the pump or extrude out of the suppressor, contaminating the system. From the figures, it can be seen that the best liner composition, in terms of material compatibility is VT-10-0-1-50-0-N-L, Figure 21 – Repeated transmission loss measurements at 4.14 MPa for a third-generation liner-style suppressor with the liner VT-10-0-1-50-0-N-L., as the suppressor containing that liner did not have any significant changes in transmission loss over repeated tests.

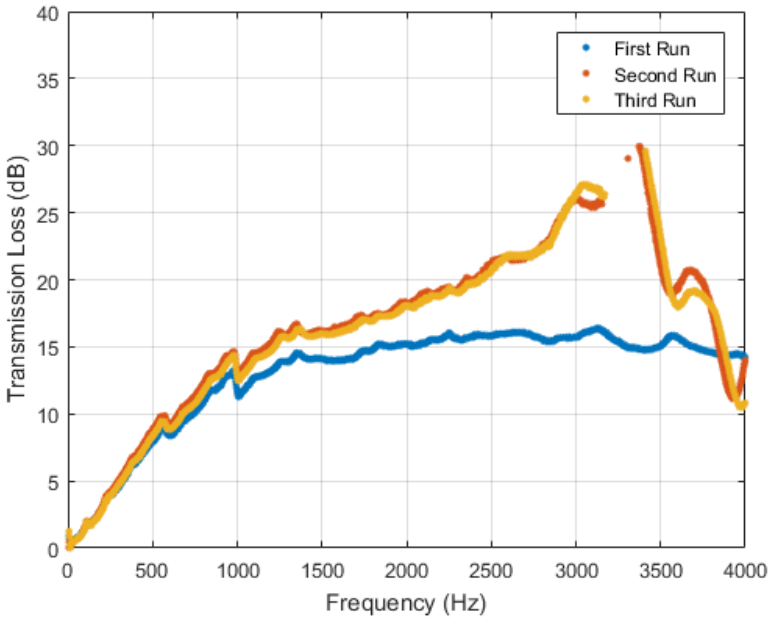

Figure 19 – Repeated transmission loss measurements at 4.14 MPa for a third-generation liner-style suppressor with the liner VT-0-0-1-50-0-N-L.

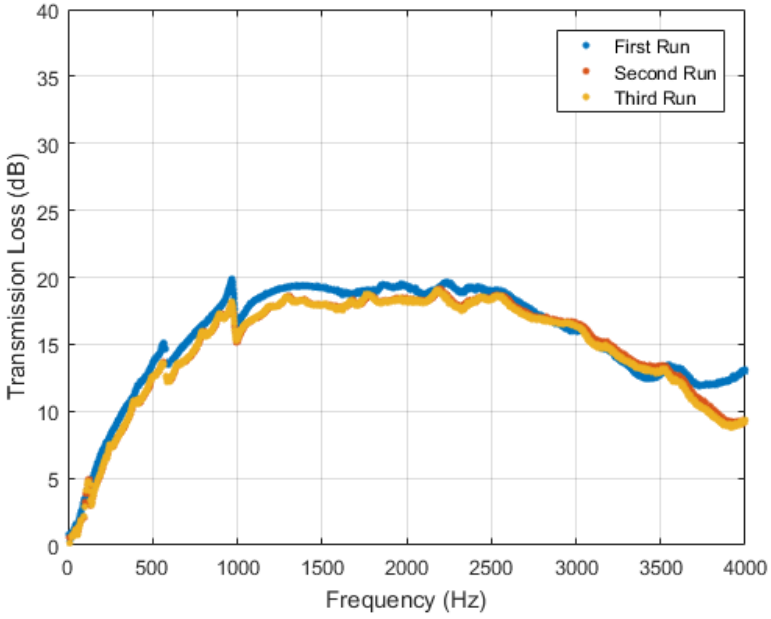

Figure 20 – Repeated transmission loss measurements at 4.14 MPa for a third-generation liner-style suppressor with the liner VT-5-0-1-50-0-N-L.

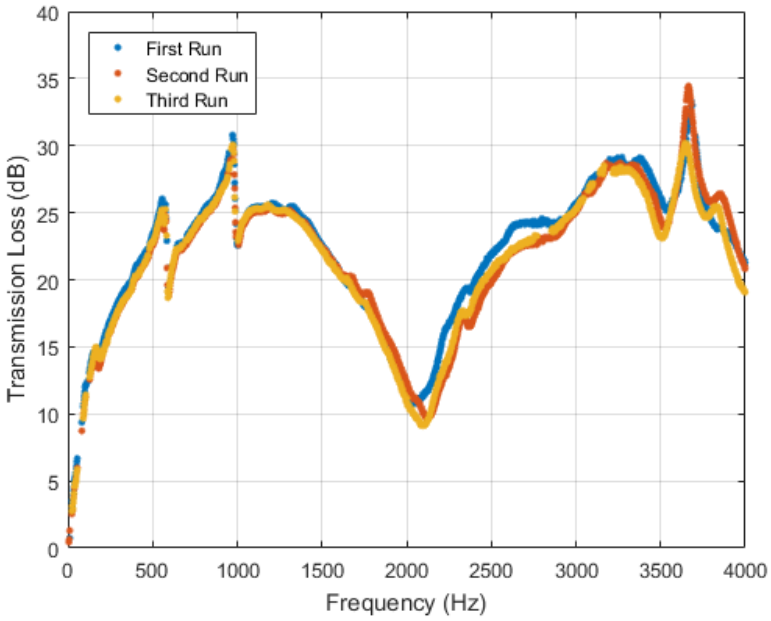

Figure 21 – Repeated transmission loss measurements at 4.14 MPa for a third-generation liner-style suppressor with the liner VT-10-0-1-50-0-N-L.

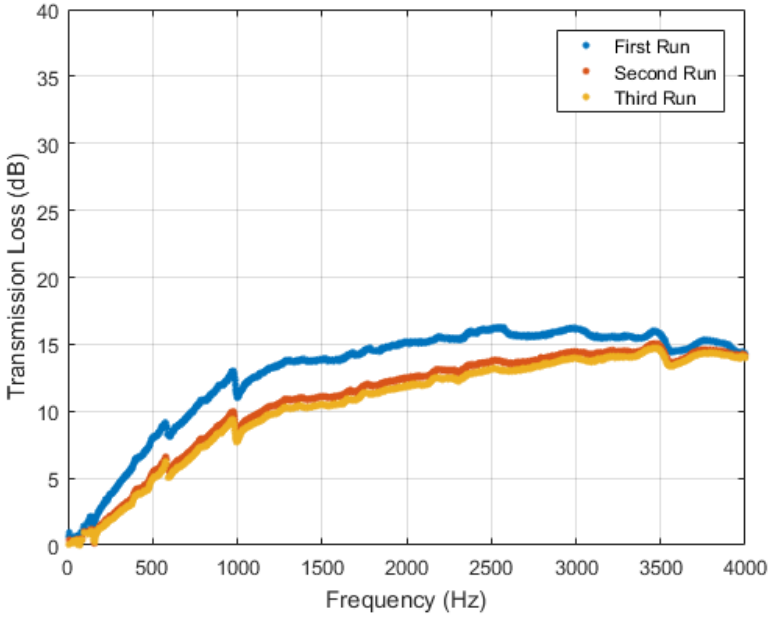

Figure 22 – Repeated transmission loss measurements at 4.14 MPa for a third-generation liner-style suppressor with the liner VT-0-1-1-50-0-N-L.

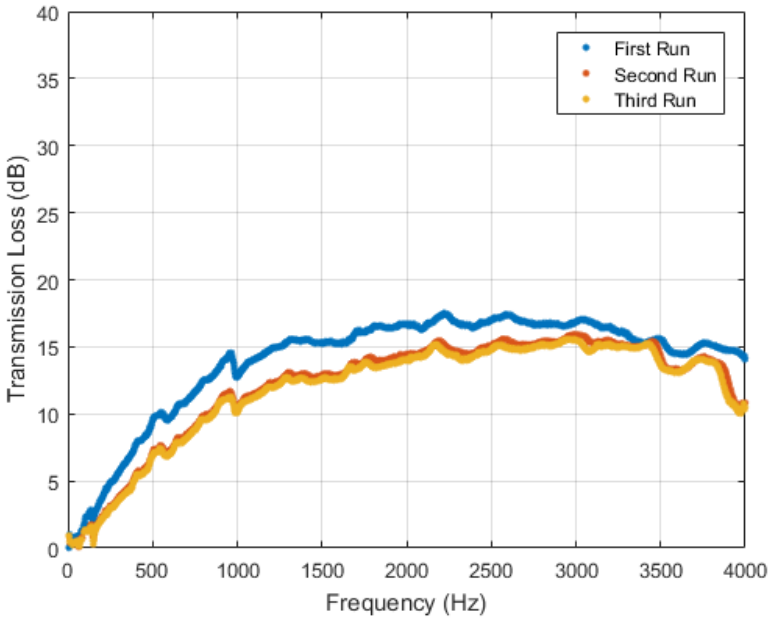

Figure 23 – Repeated transmission loss measurements at 4.14 MPa for a third-generation liner-style suppressor with the liner VT-0-2-1-50-0-N-L.

Suppressors containing VT-5-0-1-50-0-N-L, VT-0-1-1-50-0-N-L, and VT-0-2-1-50-0-N-L composition liners experienced a reduction in transmission loss indicating that they are inappropriate chemistries for the hydraulic environment. The suppressor with the VT-0-0-1-50-0-N-L composition exhibited an increase in transmission loss indicating that this foam composition is not appropriate for the hydraulic environment. The suppressor with the VT-10-0-1-50-0-N-L composition exhibited no change in transmission loss indicating that this foam composition may be appropriate for the hydraulic environment. Table 5 summarizes the material compatibility

Table 5 - Material compatibility based on observed changes in transmission loss measurements over repeated tests.

Material	Compatibility in hydraulic environment
VT-0-0-1-50-0-N-L	No
VT-5-0-1-50-0-N-L	No

VT-10-0-1-50-0-N-L	Yes
VT-0-1-1-50-0-N-L	No
VT-0-2-1-50-0-N-L	No

5.3.3.2 First Exposure

Figure 24 – First exposure transmission loss measurements of the liner-style suppressor containing VT-10-0-1-50-0-N-L at various system pressures. shows the results of the first exposure tests for the third-generation liner-style suppressor with the liner VT-10-0-1-50-0-N-L. It can be seen that acoustic performance falls off as the system pressure increases, which is consistent with theory as the bulk modulus in the suppressor should approach a constant asymptotically as the pressure increases.

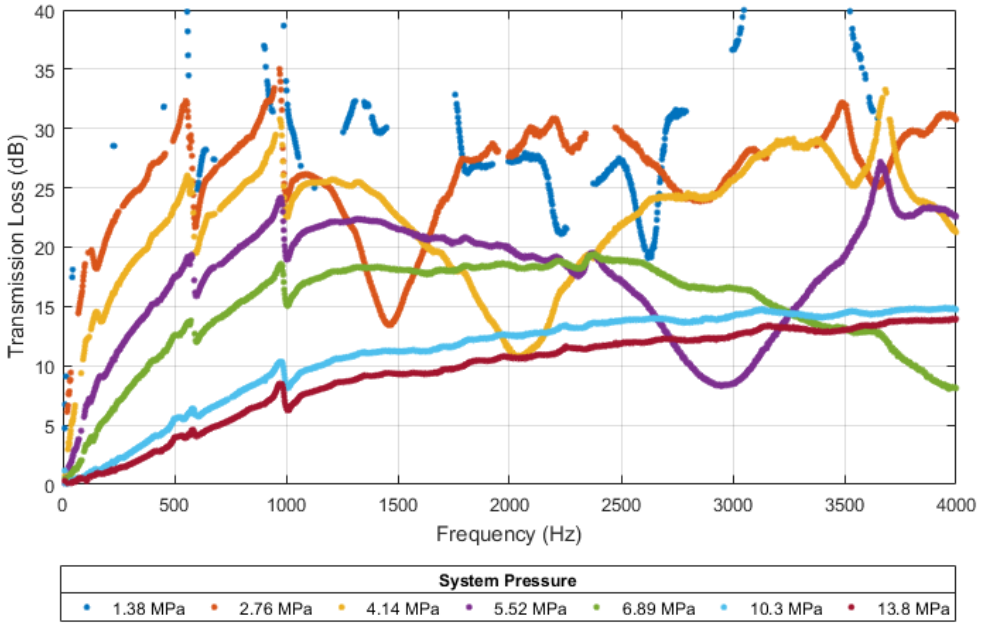

Figure 24 – First exposure transmission loss measurements of the liner-style suppressor containing VT-10-0-1-50-0-N-L at various system pressures.

5.3.4 Generational Suppressor Comparisons

Comparisons of the transmission losses of suppressors containing a GR9-625 liner (first-generation liner-style suppressor) and a VT-10-0-1-50-0-N-L liner (best performing third-generation liner-style suppressor, in terms of material compatibility) can be seen in Figures 25 through 29. From Figure 25 It can be seen that the performance of the two generations of liner-style suppressors is performance below 1250 Hz. Above 1250 Hz, the relative performance of the suppressors containing the VT-10-0-1-50-0-N-L liner and the GR9-625 liner varies greatly. It can be seen from Figures 26 to 28 that the third-generation liner-style suppressor performed better than the first-generation liner-style suppressor in the pressure range of 4.14 to 6.89 MPa for most frequencies below 4000 Hz. From Figure 29 it can be seen that above 6.89 MPa the performance of the two generations of liner-style suppressors is essentially the same.

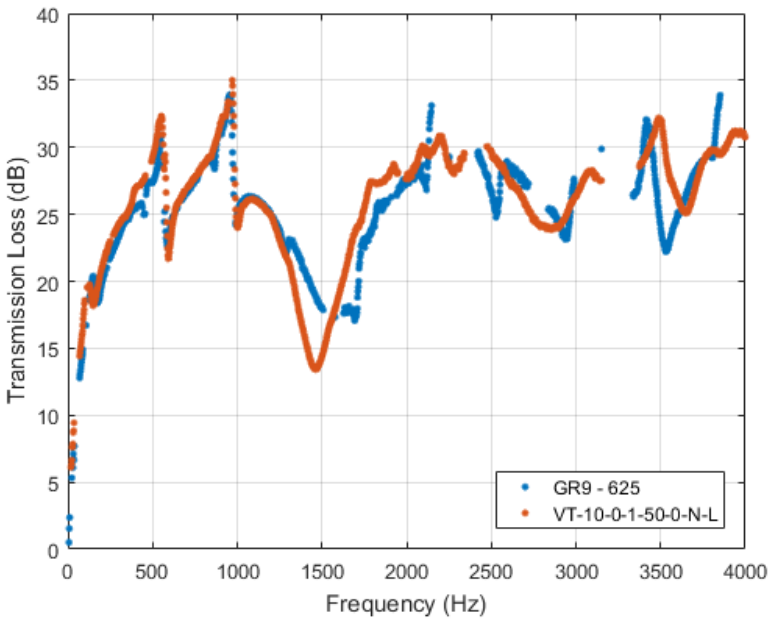

Figure 25 – Transmission loss measurements at 2.76 MPa for suppressors containing GR9-625 and VT-10-0-1-50-0-N-L liners.

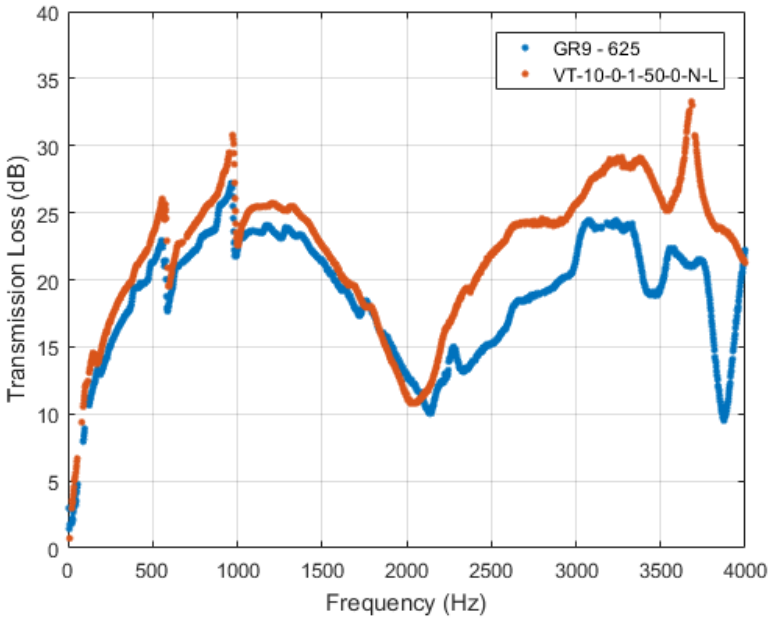

Figure 26 – Transmission loss measurements at 4.14 MPa for suppressors containing GR9-625 and VT-10-0-1-50-0-N-L liners.

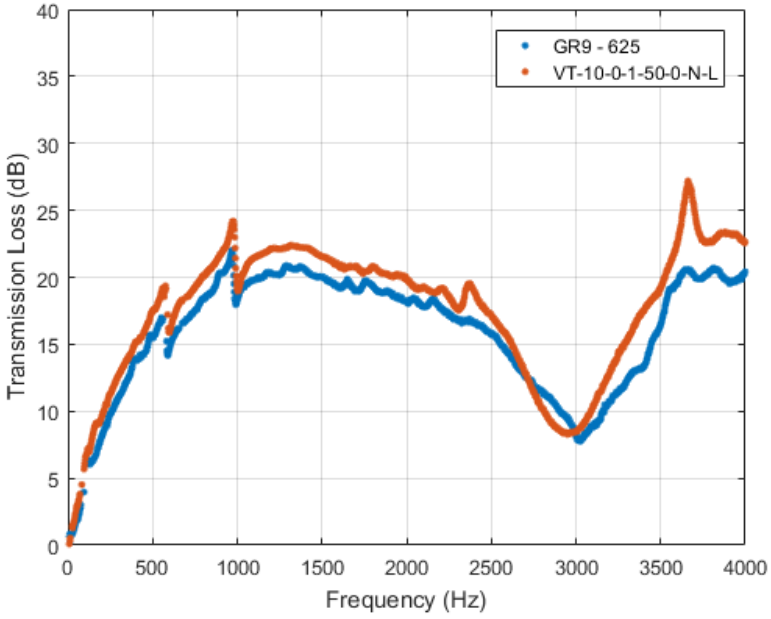

Figure 27 – Transmission loss measurements at 5.52 MPa for suppressors containing GR9-625 and VT-10-0-1-50-0-N-L liners.

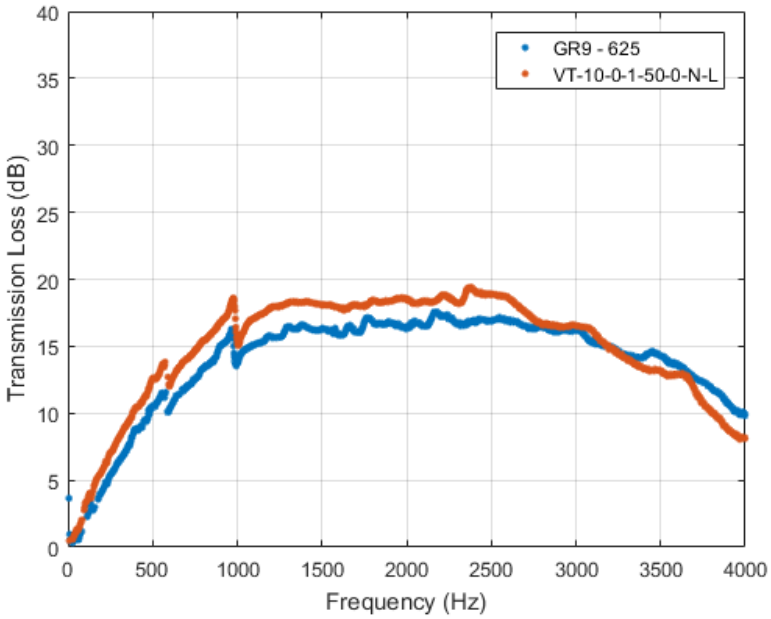

Figure 28 – Transmission loss measurements at 6.89 MPa for suppressors containing GR9-625 and VT-10-0-1-50-0-N-L liners.

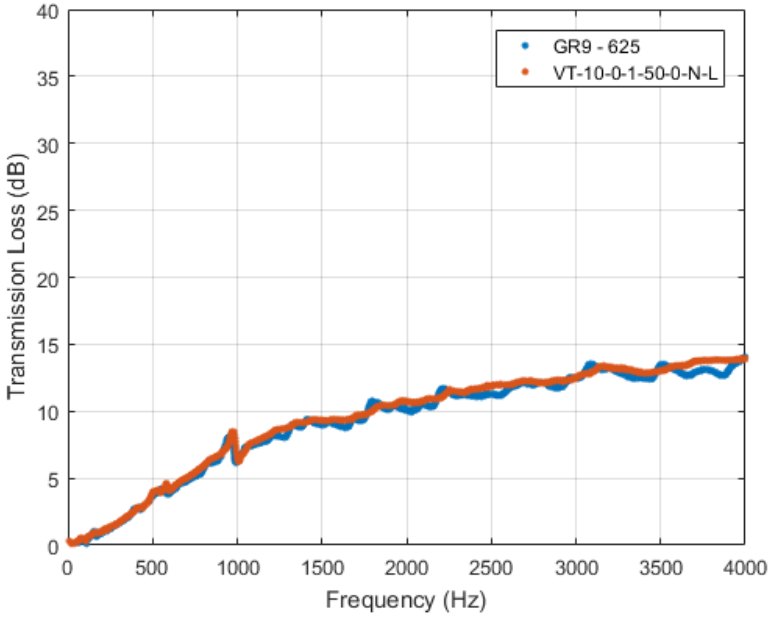

Figure 29 – Transmission loss measurements at 13.8 MPa for suppressors containing GR9-625 and VT-10-0-1-50-0-N-L liners.

CHAPTER 6. CONCLUSIONS

Syntactic foam liners for use in third-generation of liner-style hydraulic suppressors were developed that took advantage of improvements in syntactic foam technology. The use of a diffuser was considered for liner-style suppressors and found to be inadvisable. The effects of the initial volume fraction, initial microsphere pressurization, and material composition were considered for their impact on the acoustic performance of the suppressor and material compatibility.

Diffusers are not generally recommended for use with liner-style foams, as it is possible for the liner to seize on to the diffuser. The liner seizing onto the diffuser will dramatically reduce the ability of the suppressor to act as a noise reduction device and the fluid-born noise will only be exposed to small portions of the liner which will cause the suppressor to behave similarly to a stiff walled pipe. The pressures and geometries for which this seizing will occur are governed by the effective Young's modulus and Poisson's ratio of the syntactic foam, which will change with the pressure in the suppressor.

6.1 Influence of Constituent Properties on the Syntactic Foam Liner

Using commercially available microspheres, it was proven that increasing the initial volume fraction of microspheres in the liner increased the acoustic performance of the suppressor, consistent with research performed by Gruber [1]. Likewise, testing showed that increasing the initial microsphere pressurization of the microspheres in the foam significantly increased the acoustic performance of the suppressor.

The third-generation liner-style suppressor with the best acoustic performance and material compatibility used the VT-10-0-1-50-0-N-L liner. The third-generation liner-

style suppressor using the VT-10-0-1-50-0-N-L liner had comparable performance with the first-generation liner-style suppressor.

Based on the data presented in this paper it is suggested that a liner be created with 55% VF, 50 psi IMP, and 10 weight percent of additive in A. Such a liner is feasible with the current manufacturing process, with the VF and IMP being the maximum that can be achieved with current manufacturing processes. A third-generation liner-style suppressor using a liner of that composition should have acoustic performance that exceeds that of the third-generation liner-style suppressor using the VT-10-0-1-50-0-N-L liner.

6.2 Future Work

Additional work should be done to increase the material compatibility of the host matrix to the hydraulic environment, such as exploring higher weight percentages of the additive in A and transitioning to a polyester foam. Different designs of the microspheres, in terms of both chemistry and structure, should be explored that allow for an increased T_g and increased IMP. Foam geometries should be explored that allow for a greater volume of the suppressor to be occupied by foam while still allowing through flow of oil.

APPENDIX A. POLYMER COMPOSITION OF LINERS USED IN THIRD-GENERATION LINER-STYLE SUPRESSORS

The host matrix of the third generation of syntactic foam liners is a two-part polyurethane, with Side A being composed of an isocyanate and Side B being composed of a polyol. Side A is composed primarily of Vibrathane B625, which is a polyether MDI-terminated polyurethane. Isonate can be added to the Vibrathane B625 which will decrease the Side A viscosity, making it easier to mix in the microspheres, but increasing the foam hardness. Side B is composed primarily of polytetramethylene ether glycol (PTMEG) 1000, which is a polyol. Trimethylpropane can be added to the PTMEG 1000, which will result in a harder foam that has a greater resilience to pressure setting. A surfactant, AF-9000, is used to lower the viscosity of both sides of the polyurethane, thereby allowing microspheres to be mixed in more easily. A couple of drops – less than 1 mL – of dye can be added to Side B, to allow for a visual inspection of the quality of the mix. Both the surfactant and the dye are nonreactive and if added in small quantities will not alter the properties of the host matrix. The microspheres used are Expancel 461 DE 20 d70, which were selected for their high burst and critical pressures.

A.1 Test Article Naming Convention

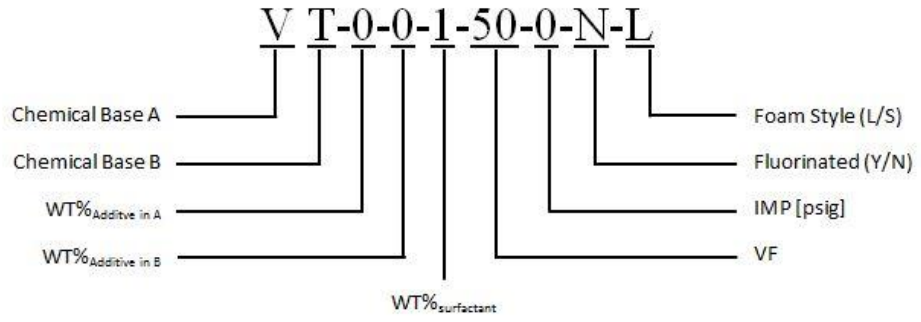

APPENDIX B. POLYMER PROCESSING PROCEDURE

The syntactic foam for the liners used in the third-generation liner-style suppressors were created using the equations and method detailed in this appendix. The specific chemical components used in the host polymer are discussed in APPENDIX A. Polymer Composition.

B.1 Polyurethane Equations

The effective weight of each component in Side A can be found as

$$EW_{component} = \frac{4200}{\%NCO_{component}} \tag{B.1}$$

where %NCO is the A measurement of the isocyanate content of the component which is reported by the manufacturer. The number 4200 used in Equation (B.1) is an industry standard number derived from polyurethane chemistry. NCO refers to a function group in which an atom of Nitrogen and an atom of oxygen are double bonded to an atom of carbon. The effective weight of each component in Side B can be found as

$$EW_{component} = \frac{56100}{OH\#_{component}} \tag{B.2}$$

where OH# is the hydroxyl group number of the polyol which is reported by the manufacturer. The number 56100 used in Equation (B.2) is an industry standard number derived from polyurethane chemistry. The effective weights of sides A and B can be found as

$$EW_X = \frac{1 - WT\%_{additive\_in\_X}}{100} \times EW_{Base_X} + \frac{WT\%_{additive\_in\_X}}{100} \times EW_{Additive_X} \quad \text{(B.3)}$$

where X denotes the side and $WT\%_{additive\_in\_X}$ is the weight percent of the additive in Side X. From this the mass ratio of A to B can be calculated as

$$\frac{m_A}{m_B} = \frac{EW_A}{EW_B} \times Iso_{adj} \quad \text{(B.4)}$$

where m_A is the mass of Side A, m_B is the mass of Side B, and Iso_{adj} is an adjustment - always a value greater than 1- to the ratio to ensure that no polyol is left unreacted. Having an Iso_{adj} greater than one will result in an isocyanate rich formulation, any isocyanate that does not react with the polyol will react with atmospheric water vapor. The weight % of each side can then be found as

$$WT\%_X = \frac{\frac{m_X}{m_B}}{\frac{m_A}{m_B} + 1} \quad \text{(B.5)}$$

where X denotes the side. The mass of each side can be found as

$$m_X = m_{Batch} \times WT\%_X \times Adj_X \quad \text{(B.6)}$$

where m_{Batch} is the mass of the batch, $WT\%_X$ is the weight percent of side X in the polyurethane and Adj_X is the mass adjustment of side X. The batch mass can be determined from the volume of the foam being cast, and is usually inflated to a certain extent so that not all of the foam needs to be scraped out of the mixing cup. The mass of Side A is not usually adjusted, but the mass of Side B is inflated by an arbitrary value –

usually between 1.1 and 1.2 – so that not all of Side B needs to be scraped out of the mixing cup. Surfactant is used to reduce the viscosity of component sides, and is generally added to the sides equally by mass. The mass of the surfactant that should be added to each side can be found as

$$m_{S,X} = m_X \times WT\%_S \tag{B.7}$$

where $WT\%_S$ is the weight percent of surfactant in the polyurethane. The mass of the microspheres can be found as

$$m_{\mu S,X} = \frac{m_X + m_{S,X}}{WT\%_X} \times WT\%_{\mu S} \times F_{\mu S\_in\_X} \tag{B.8}$$

where $WT\%_{\mu S}$ is the weight percent of microspheres in the foam, and $F_{\mu S\_in\_X}$ is the fraction of the microspheres that will be mixed into side X. The weight percent of microspheres in the foam can be found as

$$WT\%_{\mu S} = \frac{VF \times \rho_{\mu S} \times 100}{\left(\frac{WT\%_A}{\rho_A} + \frac{WT\%_B}{\rho_B}\right) \times (1 - VF)} \tag{B.9}$$

where VF is the desired volume fraction of microspheres, $\rho_{\mu S}$ is the density of the microspheres, and $\rho_{A \text{ and }} \rho_B$ are the densities of sides A and B, respectively.

B.2 Polyurethane Equations

The third generation of liners was created using the following methodology:

1. Calculate necessary masses of each component

a. Be sure to make 1.15 to 1.20 times the mass of the calculated Side B so that some may be left in the container

2. Prepare Mold
    a. If necessary, clean and spray with mold release
    b. Assemble mold and preheat in 150° F oven
3. Prepare sides A and B
    a. Prepare A side
        i. Mix appropriate masses of $Base_A$ and $Additive_A$, scraping sides and bottom of the container frequently
        ii. Stir in appropriate mass of surfactant
        iii. Place in 140° F oven until the temperature reaches 140° F
    b. Prepare B side
        i. Mix appropriate masses of $Base_B$ and $Additive_B$, scraping sides and bottom of the container frequently
        ii. Add a few drops of dye
        iii. If using $Additive_B$, heat mixture to at least 190° F
        iv. Stir in appropriate mass of surfactant
        v. If temperature has dropped below 140° F, place in 140° F oven until the temperature reaches 140° F
4. First Degassing
    a. Place both sides into the vacuum chamber at the same time; mixing sticks must not be left standing in the mixtures
    b. Close vacuum chamber and clamp lid on

c. Turn on vacuum pump

d. Expose to sub-1 torr vacuum for at least 2 minutes

e. Remove both sides from vacuum chamber and place back into oven until the temperature reaches 140° F

5. Microspheres

a. Add appropriate mass of microspheres to the A and B sides

b. Slowly mix in microspheres, scraping edges of container frequently

6. Second Degassing

a. Place both sides into the vacuum chamber at the same time; mixing sticks must not be left standing in the mixtures

b. Close vacuum chamber and clamp lid on

c. Turn on vacuum pump

d. Expose to vacuum for 15 minutes

e. Remove both sides from vacuum chamber and place back into oven until the temperature reaches 140° F

7. Mix Sides

a. Measure out correct mass of Side B into Side A container

b. Star timer

c. Using the Side A mixing stick, gently fold Side B into Side A, scraping sides and bottom of the container frequently until the mixture is homogenous

8. Pouring

a. Remove the center rod of the mold, if applicable

b. Pour the mixed foam into the mold, scraping as much of mixture as possible out of the mixing container and off the mixing stick

9. Final Degassing
    a. Sprinkle the top of the mod with a few drops of the
    b. Place mold into vacuum chamber
    c. Close vacuum chamber and clamp lid on
    d. Turn on vacuum pump
    e. Expose to vacuum for 30 minutes, or until the top of the foam ceases to move
    f. Remove from vacuum chamber
10. Center Rod
    a. Slowly insert center rod using a twisting motion to prevent pulling air into the foam
    b. Attach locating device to the top of the mold
11. Curing
    a. Reduce oven temperature to 140° F ad cure in oven for at least 16 hours
    b. Remove from oven and allow to cure at room temperature for at least 14 days before using foam

APPENDIX C. MATLAB CODES

The codes contained in this appendix are used for processing the data collected in testing and for the creation of plots to communicate the results to technical and non-technical audiences.

C.1 Transmission Loss Data Processing Codes

Two codes were used to determine the transmission loss and give an indication of the validity of the results. The transmission loss was evaluated using the Transmission Loss Code, and the Speed of Sound Function was used to indicate if the observed speed of sound matches the theoretical speed of sound in the oil. If the observed speed of sound does not match the theoretical speed of sound, the transmission loss calculations should be considered suspect.

C.1.1 Transmission Loss Code

This code evaluates and plots the transmission loss as a function of frequency in Hz, using the composite transfer functions gathered in testing [Elliott's Dissertation]. Results in this format are the most useful method for evaluating the effectiveness of the suppressor as a noise control device.

```
%% Title Section
% Program to Determine:
% - The speed of sound in hydraulic fluid
% - The reflection coefficient and apparent transmission loss (3-mic)
% - The transmission loss through transfer matrix parameters
%
% By: Nathaniel Pedigo
%
% Last Revision: 11/20/2017
%-------------------------------------------------------------------------
```

```
% function [output5 header] = TL_func(runname)

% load(run01)


clear
% close all
clc
%
%newpath = '\2012-06-08 Data WM-5081 25C Varied';
%path(path,[pwd,newpath])
%
load Check1500
showplots = 0; % 1=Yes 0=No
coher = 0.95;%0.95;
calset = 4;

% Pipe properties
I01 = 0.47; % [m] distance between sensors 0 and 1
I12 = 0.33; % [m] distance between sensors 1 and 2
I34 = 0.33; % [m] distance between sensors 3 and 4
I45 = 0.47; % [m] distance between sensors 4 and 5
%d = 0.0381; % [m] pipe inner diameter high flow system
d = 0.0206; % [m] pipe inner diameter
r0 = d / 2; % [m] pipe inner radius
%t = 0.0206; % [m] Wall thickness of the pipe
t = 0.0087376; % [m] Wall thickness of the pipe
Ew = 210e9; % [Pa] Young's modulus of the steel pipe wall

pipepropsup=struct('I01',I01,'I12',I12,'d',d,'r0',d/2,'t',t,'Ew',Ew);
pipepropsdown=struct('I01',I34,'I12',I45,'d',d,'r0',d/2,'t',t,'Ew',Ew);

% Fluid properties

% Conoco Megaflow AW ISO 46 Hydraulic Oil
% cSt @ 40degC = 46.0     (1 cSt = 10^-6 m^2/sec)
% cSt @ 100degC = 6.8
% Specific gravity @ 60degF 0.868
% Density @ 60degF = 7.23 lbs/gal

Oil_Temp = 70; %mean(TempArray0F(1:30));
Liner_Temp = 70; %mean(TempArray0C(1:30));

% kinematic viscosity
visc = 164.52e-6*exp(-0.032*Oil_Temp);
c0 = 1400; % [m/s] initial speed of sound guess
Df = 1724e6; % [Pa] Bulk modulus of the hydraulic oil
Rho = 868; % [kg/m^3] Density of hydraulic oil

fluidprops = struct('visc',visc,'Df',Df,'Ew',Ew,'Rho',Rho);
lastrow = length(TF(:,1));

Freq = transpose(Freq);
```

```
omega = Freq(:,1)*2*pi; % [rad/sec] radial frequency interval vector

% Calibrate Data
% Calibrate the transfer functions
[h01,h21,h31,h41,h51,h34,h54,ccup,ccacross,ccdown,cc] = ...
    CAL_func(TF,Power,coher);

% Compute Speed of Sound
fprintf('Upstream SOS\n')
cu = SOS_func(omega,h01,h21,pipepropsup,fluidprops,c0);

fprintf('Downstream SOS\n')
cd = SOS_func(omega,h34,h54,pipepropsdown,fluidprops,c0);


% Calculate, R, ATL, TL

% ************************************************************************
%                                 ___________
%_________________________________|           |_____________________________________
%_________________________________             _____________________________________
%  |       |        |       |___________|       |         |           |
%
%  0       1        2                           3         4           5
%  x0      x1       x2                          y0        y1          y2
%               x ---------->|          |--------> y
%                          x=0       y=0
%************************************************************************

% 0.139 is the distance from the test section to the resonator neck

x2 = -0.275;
x1 = x2 - I12;
x0  = x1 - I01;

y0 = 0.275;
y1 = y0 + I34;
y2 = y1 + I45;
Lp = 1.339 + 0.139 + .07; % Pipe length + resonator pipe + fitting to
                          % internals of termination silencer


H01(1,1,:) = h01(:,1);
H11(1,1,1:lastrow) = 1;
H21(1,1,:) = h21(:,1);

H31(1,1,:) = h31(:,1);
H41(1,1,:) = h41(:,1);
H51(1,1,:) = h51(:,1);

zeta = 1 + sqrt(visc./(r0^2*1i*omega)) + visc./(r0^2*1i*omega);

ku(1,1,:) = (omega / cu) .* zeta;   kd(1,1,:) = (omega / cd) .* zeta;

Z0u = (Rho * cu * zeta) / (pi * r0^2);
```

```
Z0d = (Rho * cd * zeta) / (pi * r0^2);

A = [exp(-1i*ku*x2) exp(1i*ku*x2);
     exp(-1i*ku*x1) exp(1i*ku*x1);
     exp(-1i*ku*x0) exp(1i*ku*x0)];
e = [H21; H11; H01];

G = [exp(-1i*kd*y0) exp(1i*kd*y0);
     exp(-1i*kd*y1) exp(1i*kd*y1);
     exp(-1i*kd*y2) exp(1i*kd*y2)];
h = [H31; H41; H51];

x = zeros(lastrow,2);
y = zeros(lastrow,2);
condx = zeros(lastrow,1);
condy = zeros(lastrow,1);

for p = 1:lastrow
    x(p,:) = transpose(pinv(A(:,:,p)) * e(:,:,p));
    condx(p,:) = cond(A(:,:,p));
    y(p,:) = transpose(pinv(G(:,:,p)) * h(:,:,p));
    condy(p,:) = cond(G(:,:,p));
end

% Preallocate matrices
Freq2 = zeros(sum(ccup),1); R = Freq2;
output2 = zeros(sum(ccup),4);

count = 1;
for ii = 1:lastrow
    if (ccup(ii) == 0);
    else
        Freq2(count,1) = Freq(ii);
        % Silencer entrance reflection coefficient
        R(count) = x(ii,2) / x(ii,1);
        output2(count,1:4) = [real(x(ii,1)),imag(x(ii,1)),...
            real(x(ii,2)),imag(x(ii,2))];
        count = count + 1;
    end
end

% Preallocate matrices
Freq4 = zeros(sum(ccdown),1);
output3 = zeros(sum(ccdown),4);

count3 = 1;
for ii = 1:lastrow
    if (ccdown(ii) == 0);
    else
        Freq4(count3,1) = Freq(ii);
        output3(count3,1:4) = [real(y(ii,1)),imag(y(ii,1)),...
            real(y(ii,2)),imag(y(ii,2))];
        count3 = count3 + 1;
    end
end
```

```
realR(:,1) = real(R);
imagR(:,1) = imag(R);
R2(:,1) = abs(R).^2; % Power reflection coefficient

Z = Rho*cu*((1 + R) ./ (1 - R)); % Silencer entrance impedance


% Generate the Transfer Matrix
p0 = x(:,1) + x(:,2); % Pressure at silencer entrance
q0 = (x(:,1) - x(:,2)) ./ Z0u; % Velocity at silencer entrance

pd = y(:,1) + y(:,2); % Pressure at silencer exit
qd = (y(:,1) - y(:,2)) ./ Z0d; % Velocity at silencer exit
% Velocity at silencer exit, different convention
% qd2 = (-y(:,1) + y(:,2)) ./ Z0d;

% pd = y(:,1);
% qd = y(:,1) ./ Z0d;

% Transfer matrix parameters
T11 = (pd .* qd + p0 .* q0) ./ (p0 .* qd + pd .* q0);
T12 = (p0.^2 - pd.^2) ./ (p0 .* qd + pd .* q0);
T21 = (q0.^2 - qd.^2) ./ (p0 .* qd + pd .* q0);
T22 = T11;

% T11 = (p0 .* qd + pd .* q0) ./ (pd .* qd + p0 .* q0);
% T12 = (p0 .* qd + pd .* q0) ./ (p0.^2 - pd.^2);
% T21 = (p0 .* qd + pd .* q0) ./ (q0.^2 - qd.^2);
% T22 = T11;

z11 = (pd.*qd - p0.*q0)./(qd.^2 - q0.^2); % = z22
z12 = (p0.*qd - pd.*q0)./(qd.^2 - q0.^2); % = z21

z11amp = abs(z11);
z11pha = angle(z11)*180/pi;
z12amp = abs(z12);
z12pha = angle(z12)*180/pi;

% Reflection coefficient at entrance of downstream pipe
Rd = y(:,2) ./ y(:,1);
% kd2 = (omega / cd) .* zeta;
% Termination silencer reflection coefficient
% Rt(:,1) = (y(:,2).*exp(-1i*kd2*Lp)) ./ (y(:,1).*exp(1i*kd2*Lp));
% Zt = Rho*cd*((1 + Rt) ./ (1 - Rt)); % Silencer entrance impedance
% Relationship btw C and D at downstream face of silencer under test
% Y(:,1) = abs(Rt .* exp(-2*1i*kd2*Lp));
% Y(:,1) = y(:,2) ./ y(:,1);

% Relative to amplitude of wave A
waveA = log10(abs(x(:,1))./abs(x(:,1)));
waveB = log10(abs(x(:,2))./abs(x(:,1)));
waveD = log10(abs(y(:,1))./abs(x(:,1)));
waveE = log10(abs(y(:,2))./abs(x(:,1)));
```

```
phaBA = angle(x(:,2)./x(:,1));
phaDC = angle(y(:,2)./y(:,1));
% diff = phaDC + phaBA;
waveratio = (x(:,2).*y(:,2))./(x(:,1).*y(:,1));
phadiff = angle(waveratio);

ccpha = ones(1,2560);%(phadiff < -.6) | (phadiff > .6);

Traveling_up = abs(x(:,1) - x(:,2).*exp(1i*phaBA));
Standing_up = abs(2*x(:,2).*exp(1i*phaBA));

Traveling_down = abs(y(:,1) - y(:,2).*exp(1i*phaDC));
Standing_down = abs(2*y(:,2).*exp(1i*phaDC));

% Preallocate matrices
Freq3 = zeros(sum(cc),1); TL = Freq3; TL1 = Freq3; TL2 = Freq3;
TL3 = Freq3; TL4 = Freq3; TL22 = Freq3;

count2 = 1;
for ii = 1:lastrow
    if (cc(ii) == 0) || (ccpha(ii) == 0)
    else
        Freq3(count2,1) = Freq(ii);

        T11(ii) = T11(ii) .* cc(ii);
        T12(ii) = T12(ii) .* cc(ii);
        T21(ii) = T21(ii) .* cc(ii);
        T22(ii) = T22(ii) .* cc(ii);

        t1 = sqrt(Z0d(ii)/Z0u(ii))*T11(ii);
        t2 = T12(ii)/sqrt(Z0u(ii)*Z0d(ii));
        t3 = sqrt(Z0u(ii)*Z0d(ii))*T21(ii);
        t4 = sqrt(Z0u(ii)/Z0d(ii))*T22(ii);

        % System-independent TL
        TL(count2,1) = 20*(log10((1/2)*abs(t1 + t2 + t3 + t4)));

        TL1(count2,1) = 20*log10((1/2)*abs(t1));
        TL2(count2,1) = 20*log10((1/2)*abs(t2));
        TL3(count2,1) = 20*log10((1/2)*abs(t3));
        TL4(count2,1) = 20*log10((1/2)*abs(t4));

        % System-dependent TL
        TL22(count2,1) = 20*log10((1/2)*abs(t1 + t2 + t3 + t4 + ...
            Rd(ii).*(t1 - t2 + t3 - t4)));

        count2 = count2 + 1;
    end
end

% figure(6);subplot(3,1,1);plot(Freq3,TL1,Freq3,TL);subplot(3,1,2);...
%     plot(Freq3,TL2,Freq3,TL);subplot(3,1,3);plot(Freq3,TL3,Freq3,TL)
```

```
% Transmission loss using impedance parameters
% TL_imped = 20*log10(0.5*abs(z11./z21 + z22./z21 + ...
%     (z11.*z22)./(z21.*Z0) + Z0./z21 - z12./Z0));%.* cc';

figure
plot(Freq3,TL,'.')
xlabel('Frequency (Hz)')
ylabel('Transmission Loss (dB)')
axis([0,4000,0,40])
```

C.1.2 Speed of Sound Function

This code evaluates the speed of sound in the upstream and downstream portions of the test section which is useful for determining the validity of the measured transmission loss.

```
% Title Section
% User-Defined Function to Determine
%  - The speed of sound for a given section of pipe
%
% By: Nicholas E. Earnhart
%
% Last Revision: 10/08/2010
%-------------------------------------------------------------------------
----

function [c] = SOS_func(omega,h01,h21,pipeprops,fluidprops,c0)

% Pipe properties
I01 = pipeprops.I01; % [m] distance between sensors 0 and 1
I12 = pipeprops.I12; % [m] distance between sensors 1 and 2
d = pipeprops.d; % [m] pipe inner diameter
r0 = pipeprops.r0; % [m] pipe inner radius
t = pipeprops.t; % [m] Wall thickness of the pipe
Ew = pipeprops.Ew; % [Pa] Young's modulus of the steel pipe wall

% Fluid properties
visc = fluidprops.visc; % [m^2/sec] kinematic viscosity
Df = fluidprops.Df; % [Pa] Bulk modulus of the hydraulic oil
Rho = fluidprops.Rho; % [kg/m^3] Density of hydraulic oil

% Script settings
m = 1; % [ND] For loop index
coher = 0.90; % [ND] value for coherence to be valid
g = 0; % [ND] 1 = display graphics for SOS, 0 = no graphics

% Determination of the velocity of the wave propagation pulsations
(speed
% of sound) in a fluid enclosed by a homogeneous and straight pipe
using
```

```
% the three pressure transducer - method 1 - transducer 2 between 1 and
3
%  c       final value speed of sound                              [m/s]
%  I01     distance between pressure transducers 1 and 2           [m]
%  I12     distance between pressure transducers 2 and 3           [m]
%  d       inside diameter of the rigid pipe                       [m]
%  visc    kinematic viscosity of the fluid at test conditions     [m^2/s]
%  c0      initial chosen value of the speed of sound              [m/2]
%  omega   (2*pi*f) vector of individual freq. used in msmts [rad/sec]
%
%  h01,h21
%          2 dimensional matrices containing respectively, the transfer
%          functions P1/P2 and associated coherence; and P2/P1 and
%          associated coherence. that is h01(:,1) and h21(:,1) contain
the
%          transfer function in complex number format and h01(:,2) and
%          h21(:,2) contain corresponding real number choerences. These
%          matrices are of the same length as the omega vector.
%
%  coher   min value for coherence for msmts to be valid (typ.
coher=.95)
%  g       printing option (text and graphics on screen is g==1)

% Now must input the transfer function data in magnitude and phase form
% and convert it to complex notation to be passed to the function. Must
do
% this for both workspaces imported into the m-file.


% -------- LOOKING FOR AVALIABLE FREQUENCIES  (coherence > min value)
nrc = 0; % Initialize the number of available frequencies

for nc = 1:length(omega)
    if (h01(nc,2) * h21(nc,2) >= coher*coher)
        nrc = nrc + 1;
        nv(nc) = 1;  % Index the available frequencies
    else
        nv(nc) = 0;  % Index the unavailable frequencies
    end
end

nv(1) = 0;  % Null frequencies not taken into account


%------BEGINING OF THE LOOP ALGORTIHM------
a = omega + sqrt(2 * omega * visc) / d;
b = (4 * visc) / (d * d) + sqrt(2 * omega * visc) / d;

amjb = a - 1i*b;

I01xamjb = I01 * amjb;
I12xamjb = I12 * amjb;

ik = 1; % Initialize number of iterations of the algorithm
```

```
c = c0;
dc = 10;

while (abs(dc / c) > 0.0001)
memc(ik) = c;   % Memorize num of successive values for opt
observations
I01_ = I01xamjb / c;
I12_ = I12xamjb / c;

E = nv(:).*(sin(I12_).*h01(:,1)+sin(I01_).*h21(:,1)-sin(I01_+I12_));
dEsurdc = nv(:).*amjb/(c*c).*(-I12*cos(I12_).*h01(:,1)-
I01*cos(I01_).*...
    h21(:,1)+(I01+I12)*cos(I01_+I12_));

dc = -sum(E .* conj(dEsurdc)) / sum(dEsurdc .* conj(dEsurdc));
dc = real(dc); % real: force c to be real value
c = abs(c + dc); % abs: force c to be positive value


%--------TEXTS ON SCREEN--------
if (g == 1) && (ik == 1)
    fprintf('\nDetermination of Speed of Sound with ');
    fprintf('Coherence Imposed. %g\n', coher);
    fprintf('Number of Available Frequencies: ');
    fprintf('%g on %g maximum\n', nrc, length(omega));
    fprintf('c%g=%6.2f dc=%6.4f\n',ik, c0, dc);
else
    fprintf('c%g=%6.2f dc=%6.4f\n', ik, memc(ik), dc);
end


%--------WARNING MESSAGE--------
if (ik > 50)
   fprintf('Number of Iteration Values > 50\n');
   fprintf('Something is Wrong! Verify the Initial Values\n');
   return
end

ik = ik + 1;   % Increment the Number of Iterations
end

%-------------------------------------------------------------------------
----
%----------------------------- CORRECTION TEST ----------------------
----
%-------------------------------------------------------------------------
----

% Need to see if the stiffness of the steel wall relative to the bulk
% modulus of the fluid is a small enough ratio to warrant correction of
the
% bulk modulus of the fluid

Dc = Df / (1 + (d/2) / t * Df / Ew);
```

```
% Theoretical SOS:
ctheo = sqrt(Dc / Rho);


%--------GRAPHICS--------
fprintf('\nFinal Value of Speed of Sound = %6.0f m/s',real(c));
fprintf('\nTheoretical Value Speed of Sound = %6.0f
m/s\n\n',real(ctheo));

if (g == 1),
    np = 1:ik-1;
    plot(np, memc(np),'*w', np, memc(np));
    grid on;
    xlabel('Number of Iterations');
    ylabel('Speed of Sound [m/s]');
    title('Progression of the Algorithm');
    text(0.5, 0.5, ['Final Value = ', num2str(c)], 'sc');
end
```

C.2 Pressure Ripple Plotting Code

This code is used to plot the fluid-borne noise at each sensor, which is useful when attempting to communicate the results of the research to people that are not used to interpreting results in terms of decibels or in the frequency domain.

```
% Time_Trace_Plotting
% Created by: Nathaniel Pedigo
% Created on: 5/11/17
% Last Editted: 5/11/17

clear;  clc;

load run7

figure

subplot(2,3,1)
plot(Time(1:200),Voltage_0(1:200))
title('Voltage 1 - Upstream')
yl1=ylim;

subplot(2,3,2)
plot(Time(1:200),Voltage_1(1:200))
title('Voltage 2 - Upstream')
ylim(yl1)

subplot(2,3,3)
```

```
plot(Time(1:200),Voltage_2(1:200))
title('Voltage 3 - Upstream')
ylim(yl1)

subplot(2,3,4)
plot(Time(1:200),Voltage_3(1:200))
title('Voltage 4 - Downstream')
ylim(yl1)

subplot(2,3,5)
plot(Time(1:200),Voltage_4(1:200))
title('Voltage 5 - Downstream')
ylim(yl1)

subplot(2,3,6)
plot(Time(1:200),Voltage_5(1:200))
title('Voltage 6 - Downstream')
ylim(yl1)

suptitle('Time Trace of Pressure Ripple - System Pressure: 2000 psi')
```

APPENDIX D. MATHEMATICAL PROCESSING

The acoustic pressure in the up- and down- stream sections can be expressed as plane waves in traveling in the positive and negative *x*-directions. The dynamic pressure at the upstream and downstream ports of the suppressor can be calculated as

$$p_{upstream} = \left(Ae^{-\gamma x} + Be^{\gamma x} \right) e^{j\omega t} \tag{D.1}$$

and

$$p_{downstream} = \left(Ee^{-\gamma x} + Fe^{\gamma x} \right) e^{j\omega t} \tag{D.2}$$

respectively, where ω is the angular frequency of the noise, γ is the complex wavenumber, j is the imaginary number, and A, B, E, and F are the complex wave amplitudes in the upstream and downstream sections of the pipe, as shown in Figure 30.

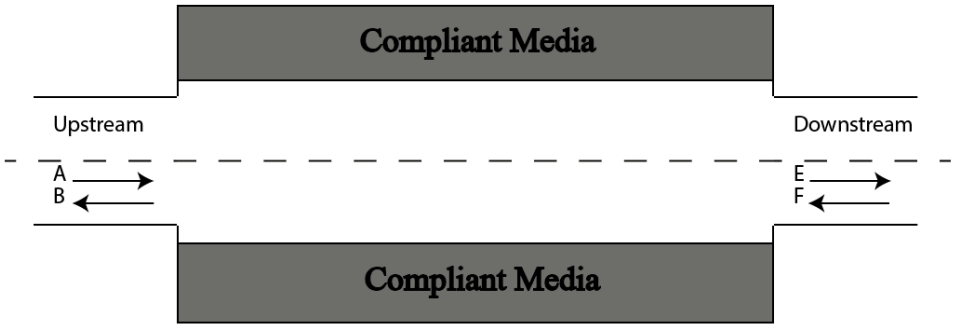

Figure 30 – Acoustic diagram of a suppressor.

Using the dynamic pressure sensors as depicted in Figure 11, the transfer function between sensors *h* and *i*, denoted by H_{hi} relates the signals measured by the two sensors. Seven transfer functions are used to fully analyse the data; the data from all of the sensors

is related to the data collected at sensor 1, and the data at sensors 3 and 5 are related to the data collected at sensor 4. The relative wave amplitudes can be determined by solving the Moor-Penrose pseudoinverses

$$X = Mb \tag{D.3}$$

and

$$Y = Nc \tag{D.4}$$

where X and Y are defined as

$$X = \begin{pmatrix} A/p_1 \\ B/p_1 \end{pmatrix} \tag{D.5}$$

and

$$Y = \begin{pmatrix} E/p_1 \\ F/p_1 \end{pmatrix} \tag{D.6}$$

respectively, where p_1 is the pressure at sensor 1. The matrices b and c are defined as

$$b = \begin{pmatrix} H_{01} \\ 1 \\ H_{21} \end{pmatrix} \tag{D.7}$$

and

$$c = \begin{pmatrix} H_{31} \\ H_{41} \\ H_{51} \end{pmatrix} \tag{D.8}$$

respectively. The measured pressures at each sensor can be placed in over-determined matrices such that

$$M = \begin{bmatrix} e^{-\gamma x_0} & e^{\gamma x_0} \\ e^{-\gamma x_1} & e^{\gamma x_1} \\ e^{-\gamma x_2} & e^{\gamma x_2} \end{bmatrix} \tag{D.9}$$

and

$$N = \begin{bmatrix} e^{-\gamma x_3} & e^{\gamma x_3} \\ e^{-\gamma x_4} & e^{\gamma x_4} \\ e^{-\gamma x_5} & e^{\gamma x5} \end{bmatrix} \tag{D.10}$$

The Moore-Penrose pseudoinverse equations, (D.3) and (D.4), can be used to calculate the complex wave amplitudes with respect to the pressure at sensor x_1. The upstream and downstream volume velocities can be calculated as

$$Q_{upstream} = \frac{\left(Ae^{-\gamma x} - Be^{\gamma x}\right)}{Z_0} e^{j\omega t} \tag{D.11}$$

and

$$Q_{downstream} = \frac{\left(Ee^{-\gamma x} - Fe^{\gamma x}\right)}{Z_0} e^{j\omega t} \tag{D.12}$$

where Z_0 is the specific acoustic impedance of the hydraulic fluid. A transfer matrix relates the pressure and volume velocities in the upstream and downstream sections such that

$$\begin{pmatrix} P_{upstream} \\ Q_{upstream} \end{pmatrix} = \begin{bmatrix} t_{11} & t_{12} \\ t_{21} & t_{22} \end{bmatrix} \begin{pmatrix} P_{downstream} \\ Q_{downstream} \end{pmatrix} \tag{D.13}$$

Assuming the geometric symmetry of the test component and that the system is acoustically reciprocal [14], it can be shown that

$$t_{11} = t_{22} \tag{D.14}$$

and

$$t_{21} = \frac{1 + t_{11}^2}{t_{12}} \tag{D.15}$$

From equations (D.13), (D.14), and (D.15) the transfer matrix can be rewritten as

$$T = \begin{bmatrix} 1 & -Z_0 \dfrac{A^2 + 2AB + B^2 - F^2 - 2EF - E^2}{A^2 + E^2 - B^2 - F^2} \\ \dfrac{-1}{Z_0} \dfrac{A^2 - 2AB + B^2 - F^2 + 2EF - E^2}{A^2 + E^2 - B^2 - F^2} & 1 \end{bmatrix} \tag{D.16}$$

The transmission loss of the device can be calculated as

$$TL = 20 \log_{10} \left(\frac{1}{2} \left| t_{11} + \frac{t_{12}}{Z_0} + Z_0 t_{21} + t_{22} \right| \right) \tag{D.17}$$

Substituting Equation (D.16) into (D.17), the transmission loss can be shown to be

$$TL = 20\log_{10}\left|\frac{A^2 - F^2}{AE - BF}\right| \tag{D.18}$$

The system cannot be assumed to be anechoic, thus no more simplification can be made.

D.1 Plane Wave Assumption

The mathematical process described in this aapendix is only valid for plane waves so that the wave field in the test section is not angularly dependent, and the angle of the transducer mounting is irrelevant. Only plane wave will propagate in a waveguide for frequencies less than

$$\omega_{lm} = c_{phase} k_{lm} \tag{D.19}$$

where c_{phase} is the phase speed of sound and k_{lm} is the acoustic wavenumber of the mode (l,m) defined by

$$k_{lm} = \frac{j'_{lm}}{a} \tag{D.20}$$

where j'_{lm} are the extrema of $J_m(z)$. $J_m(z)$ is the mth order Bessel function and a is the inner radius of the pipe [15]. The lower bound limit of Equation (D.19) is the cutoff angular frequency, above which nonplanar waves will be produced that decay exponentially with the distance from the source. For the test rig used in this research, the cutoff frequency for the first non-plane mode ($l=0$, $m=1$) is 43,000 Hz. As the maximum frequency of interest in this research is 4,000 Hz, the plane wave assumption is valid.

REFERENCES

[1] Gruber, E. R., 2016, "High-Pressure Compliant Syntactic Foam for Hydraulic Noise Control," Ph.D. thesis, Woodruff School of Mechanical Engineering, The Georgia Institute of Technology.

[2] Monaghan, M., "Racket Busters," SAE Off-Highway Engineering, 2014, pp. 25-27.

[3] Arendt, E., 1988, "Pulsation absorbing device," US, 4759387.

[4] Salmon, R. A., 2015, "Development of a Second Generation Liner-Style Hydraulic Suppressor," M.S. thesis, Woodruff School of Mechanical Engineering, The Georgia Institute of Technology.

[5] Ijas, M., and Virvalo, T., 2000, "Experimental Verification of pulsation Dampers and Their Simplified Theory," Power Transmission and Motion Control, pp. 13-27.

[6] Marek, K. A., 2012, "The Modelling and Use of Syntactic Foams for Passive control of Fluid-Borne Noise," Ph.D. thesis, Woodruff School of Mechanical Engineering, The Georgia Institute of Technology.

[7] Akzo Nobel, "Compression of Expancel DE."

[8] Bies, D. A., and Hansen, C. H., 2009, Engineering Noise Control: Fourth Edition, Spon Press, New York, NY, pp 443.

[9] Young, W. C., Budynas, R. G., Sadegh, A. M., 2012, *Roark's Formulas for Stress and Strain: Eighth Edition*, McGraw-Hill, New York, NY.

[10] Hashin, Z., "The elastic moduli of heterogeneous materials," Journal of Applied Mechanics, 1962 (29), pp. 143-150.

[11] Johnston, D. N., Drew, J. E., "A technique for the measurement of the transfer matrix characteristics of two-port hydraulic components," Fluid Power Systems and Technology, (1994) vol. 1, pp. 25-33.

[12] I.S.O., 2000, "Hydraulic fluid power – Determination of fluid-borne noise characteristics of components and systems," ISO-15086-2.

[13] I.S.O., 2008, "Hydraulic fluid power – Determination of the fluid-borne noise characteristics of components and systems," ISO-15086-3.

[14] Pierce, A. D., 1991, *Acoustics: An Introduction to Its Physical Principles and Applications*, Acoustical Society of America, Melville, NY.

[15] Kinsler, L. E., Frey, A. R., Coppens, A. B., Sanders, J. V., 2000, *Fundamentals of Acoustics: Fourth Edition, John Wiley & Sons*, New York, NY.